Available online at www.sciencedirect.com
ScienceDirect
Journal of Computational Physics 225 (2007) 1695–1720
JOURNAL OF COMPUTATIONAL PHYSICS
www.elsevier.com/locate/jcp

Methods for coupling radiation, ion, and electron energies in grey Implicit Monte Carlo

T.M. Evans *, J.D. Densmore

CCS-2, Computational Physics Group, MS D409, Los Alamos National Laboratory, Los Alamos, NM 87545, United States

Received 14 September 2006; received in revised form 5 February 2007; accepted 12 February 2007
Available online 1 March 2007

Abstract

We present three methods for extending the Implicit Monte Carlo (IMC) method to treat the time-evolution of coupled radiation, electron, and ion energies. The first method splits the ion and electron coupling and conduction from the standard IMC radiation-transport process. The second method recasts the IMC equations such that part of the coupling is treated during the Monte Carlo calculation. The third method treats all of the coupling and conduction in the Monte Carlo simulation. We apply modified equation analysis (MEA) to simplified forms of each method that neglects the errors in the conduction terms. Through MEA we show that the third method is theoretically the most accurate. We demonstrate the effectiveness of each method on a series of 0-dimensional, nonlinear benchmark problems where the accuracy of the third method is shown to be up to ten times greater than the other coupling methods for selected calculations.

Keywords: Thermal radiation transport; Implicit Monte Carlo; Three-temperature model

1. Introduction

The simulation of thermal radiation propagation ranks among the most difficult class of transport problems. These problems are highly nonlinear, and the fundamental unknown (the radiation intensity) can be a function of seven independent variables (in 3D). One of the most successful and widely used methods in thermal radiation transport is Implicit Monte Carlo (IMC) [1]. This method is a two-temperature (2T) scheme that includes radiation and material coupling where the matter is represented by a single temperature.

A more accurate description of the radiation and material coupling represents the ions and electrons by distinct, separate temperatures [2]. The resulting three-temperature (3T) equations for the time evolution of the radiation, electron, and ion energies include terms representing electron–ion coupling and conduction [3]. Conventionally, this system of equations is solved using radiation diffusion with operator-split conduction and coupling [4]. Fully nonlinear solutions using radiation diffusion have been shown in Ref. [2].

* Corresponding author. Current address: Reactor Analysis Group, One Bethel Valley Road, PO Box 2008 MS6172, Oak Ridge National Laboratory, Oak Ridge, TN 37831, United States. Tel.: +1 865 576 3535; fax: +1 865 574 9619.
E-mail addresses: evanstm@ornl.gov (T.M. Evans), jdd@lanl.gov (J.D. Densmore).

0021-9991/$ - see front matter © 2007 Elsevier Inc. All rights reserved.
doi:10.1016/j.jcp.2007.02.020

The objective of this paper is to extend the standard, grey IMC method to include 3T physics. Descriptions of matter that include separate energies for electrons and ions are important in high energy density physics applications and astrophysics [5]. The first part of this paper will describe the 3T energy-evolution equations, as these are not common in much of the existing radiation transport literature. Next, we derive three methods for solving the 3T equations using IMC. These are presented in 3D, frequency-integrated form.

The first method uses the standard IMC technique to simulate radiation transport. The conduction and coupling terms are linearized and split into separate equations that are solved independently. A second method uses a more robust splitting scheme in which half of the coupling is treated during the transport simulation. The conduction is split from the ion and electron equations and is solved subsequently. Afterward, the second half of the coupling is solved. The third method treats the conduction explicitly and includes all of the conduction and coupling in the linearization of the transport equation. This is a good approximation when the conduction timescales are much longer than the radiation-transport timescales. We expect this to be the case for most problems because the conduction timescales are related to the electron thermal velocity whereas the radiation moves at the speed of light. The resulting system has three equations: a Monte Carlo transport equation and two decoupled energy equations for electrons and ions.

In the next part of the paper, we provide an analytical framework for determining which method performs best through modified equation analysis (MEA). MEA has been shown to be a useful technique for determining the errors that result from splitting and linearization methods [6,7]. In MEA we formulate the continuous system of equations from the discretized system using Taylor series expansions. The resulting system of equations gives the continuous system plus the error terms that are imposed by a particular splitting or linearization strategy. This *modified* system of equations can then be solved using an unsplit, nonlinear method to evaluate the error terms imposed by the discrete method. Newton iteration is commonly used to solve the unsplit systems of nonlinear equations [7].

We perform MEA on a simplified, space-independent version of the IMC equations. The validity of this approach is justified on the grounds that all of the methods will have identical error terms associated with the spatial treatment of the radiation. Furthermore, the spatial behavior of Monte Carlo methods is well-understood, although IMC has more complexity then linear Monte Carlo transport simulations due to spatial discretizations of the material temperature that can result in severe boundary-layer effects at wave fronts and material interfaces. Thus, the MEA provides a useful mechanism for analyzing the linearization and splitting errors that are different in each of the proposed IMC methods.

Naturally, the 0-dimensional nature of the analysis means that we neglect splitting errors due to conduction. Conduction is neglected from the analysis because of the complexities that are involved in performing MEA on angular and space-dependent transport equations. Based on the results of the analysis, we can infer that additional splits will add error. Therefore, the analysis is still valid for predicting trends even though the absolute magnitude of the errors will change when conduction is included. We will undertake a qualitative analysis of conduction errors in a future paper.

Finally, we validate the results of the MEA by performing a series of calculations with varying initial data. These calculations are performed on space-independent forms of the IMC equations. For similar reasons as stated above, these calculations provide justification for choosing a particular method based upon problem specification.

This paper will formulate and analyze three methods for incorporating 3T physics into an IMC simulation. In Section 2 we describe the governing equations in the 3T model. Section 3 shows derivations of the three IMC methods that solve the 3T equations. We perform MEA on simplified, space-independent versions of the IMC equations in Sections 4 and 5. We will examine the effects of linear and nonlinear material data in Section 6. Our conclusions are presented in Section 7.

2. 3T Model

We use a 3T model that includes electron–ion coupling and conduction. Electromagnetic effects are not considered. The radiation transport is split from any associated hydrodynamics effects. Thus, errors that result from splitting the radiation from the hydrodynamics are neglected. We include ion conduction as shown in Ref. [3]. The 3T system consists of radiation, electron, and ion energy equations [2,3]:

$$\frac{1}{c}\frac{\partial \psi}{\partial t} + \widehat{\mathbf{\Omega}} \cdot \nabla \psi + \sigma \psi = \sigma B(v, T_e); \tag{1}$$

$$\frac{\partial e_e}{\partial t} = \nabla \cdot D_e \nabla T_e + \frac{C_{ve}}{\tau}(T_i - T_e) + \int_{4\pi}\int_v \sigma(\psi - B(v, T_e))\,dv\,d\mathbf{\Omega} + Q_e; \tag{2}$$

$$\frac{\partial e_i}{\partial t} = \nabla \cdot D_i \nabla T_i - \frac{C_{ve}}{\tau}(T_i - T_e) + Q_i. \tag{3}$$

Here, we define the state variables and source terms as

radiation intensity $\psi \equiv \psi(\mathbf{x}, \mathbf{\Omega}, v, t)$ [GJ cm^{-2} ns^{-1} keV^{-1} str^{-1}],
internal energy $e_\alpha \equiv e_\alpha(\mathbf{x}, T, t)$ [GJ cm^{-3}],
temperature $T_\alpha \equiv T_\alpha(\mathbf{x}, t)$ [keV],
source $Q_\alpha \equiv Q_\alpha(\mathbf{x}, t)$ [GJ cm^{-3} ns^{-1}],

where $\alpha = e, i$ for electrons and ions, and v is expressed in units of hv [keV]. The independent variables are $\mathbf{x}$, $\mathbf{\Omega}$, v, and t for space, angle, frequency, and time. The speed of light is $c = 29.979$ cm ns^{-1}.

The temperature is a function of internal energy through the equation-of-state (EOS) relationship:

$$C_{v\alpha} = \frac{de_\alpha}{dT_\alpha}, \tag{4}$$

where $C_{v\alpha} \to \rho C_{v\alpha}$ is the specific heat of ions and electrons at constant density and has units of GJ cm^{-3} keV^{-1}. For convenience, we have folded the density into the definition of C_v, although this is not normal practice because density varies during a radiation-hydrodynamics calculation. The conduction terms are defined by thermal diffusion coefficients, $D_\alpha \equiv D_\alpha(\mathbf{x}, T_\alpha)$ [GJ cm^{-1} ns^{-1} keV^{-1}], that are, in general, nonlinear functions of temperature. The ion–electron coupling timescale is defined by the collisional time, $\tau \equiv \tau(\mathbf{x}, T_e)$ [ns] [3],

$$\tau = 1.08782 \times 10^{19}\frac{T_e^{3/2}}{n\lambda}. \tag{5}$$

Here, λ is the Coulomb wavelength between electrons and ions and is generally in the range $10 \leqslant \lambda \leqslant 20$, and n is the number density. We note that λ can also be defined by models with T_i dependence. The radiation–electron equilibration timescale is $(\sigma c)^{-1}$, where $\sigma \equiv \sigma(\mathbf{x}, v, T_e)$ [cm^{-1}] is the opacity

This model is valid in the local thermodynamic equilibrium (LTE) limit in which the emission of radiation can be described by the Planck function, $B \equiv B(v, T_e)$, and

$$\int B(v, T_e)\,dv = \frac{1}{4\pi}acT_e^4, \tag{6}$$

where $a = 0.01372$ GJ cm^{-3} keV^4 is the radiation constant. The spectral radiation energy density is the zeroth angular moment of the radiation intensity,

$$E(\mathbf{x}, v, t) = \frac{1}{c}\int_{4\pi} \psi(\mathbf{x}, \mathbf{\Omega}, v, t)\,d\mathbf{\Omega}. \tag{7}$$

We define the radiation temperature, T_r, in a manner that is consistent with the LTE approximation by assuming that the radiation intensity can be described by a Planckian at T_r,

$$E(\mathbf{x}, t) = \int E(\mathbf{x}, v, t)\,dv \approx \frac{1}{c}\int\int B(v, T_r)\,d\mathbf{\Omega}\,dv = aT_r^4. \tag{8}$$

In all of the work that follows we shall use the grey approximation where

$$\psi \equiv \psi(\mathbf{x}, \mathbf{\Omega}, t) = \int \psi(\mathbf{x}, \mathbf{\Omega}, v, t)\,dv,$$

$$\sigma \equiv \sigma(\mathbf{x}, T).$$

Operating on Eq. (1) by $\int(\cdot)\mathrm{d}v$ and using the preceding definitions, we derive the following coupled set of equations describing the time evolution of radiation, electron, and ion energy,

$$\frac{1}{c}\frac{\partial\psi}{\partial t}+\widehat{\mathbf{\Omega}}\cdot\nabla\psi+\sigma\psi=\frac{1}{4\pi}\sigma acT_{\mathrm{e}}^{4}, \tag{9}$$

$$\frac{\partial e_{\mathrm{e}}}{\partial t}=\nabla\cdot D_{\mathrm{e}}\nabla T_{\mathrm{e}}+\frac{C_{\mathrm{ve}}}{\tau}(T_{\mathrm{i}}-T_{\mathrm{e}})+\int\sigma\psi\,\mathrm{d}\mathbf{\Omega}-\sigma acT_{\mathrm{e}}^{4}+Q_{\mathrm{e}}, \tag{10}$$

$$\frac{\partial e_{\mathrm{i}}}{\partial t}=\nabla\cdot D_{\mathrm{i}}\nabla T_{\mathrm{i}}-\frac{C_{\mathrm{ve}}}{\tau}(T_{\mathrm{i}}-T_{\mathrm{e}})+Q_{\mathrm{i}}. \tag{11}$$

We note that $\int\sigma\psi\,\mathrm{d}\mathbf{\Omega}=\sigma cE$; however, this term is left in integral form for reasons that will become clear in Section 3.

3. 3T IMC Methods

The objective is to define IMC methods that can be used to solve the system of equations in (9)–(11). The standard IMC method [1] solves a 2T version of the model by linearizing the system through the transform

$$\frac{\partial e}{\partial t}\approx\frac{C_{\mathrm{v}}^{n}}{4a(T^{n})^{3}}\frac{\partial\phi}{\partial t}\approx\frac{1}{\beta^{n}}\frac{\phi-\phi^{n}}{\Delta t}, \tag{12}$$

where $\phi=aT^{4}$. This expression and the material-energy equation are used to develop a function for ϕ that linearizes the emission source term. The resulting IMC equations are

$$\frac{1}{c}\frac{\partial\psi}{\partial t}+\widehat{\mathbf{\Omega}}\cdot\nabla\psi+\sigma^{n}\psi=\frac{1}{4\pi}\left[f\sigma^{n}c\phi^{n}+(1-f)\left(\int\sigma^{n}\psi\,\mathrm{d}\mathbf{\Omega}+Q^{n}\right)\right], \tag{13}$$

$$\frac{\partial e}{\partial t}=f\int\sigma^{n}\psi\,\mathrm{d}\mathbf{\Omega}-f\sigma^{n}c\phi^{n}+fQ^{n}, \tag{14}$$

where f is the *Fleck factor*,

$$f=\frac{1}{1+\beta^{n}\sigma^{n}c\Delta t}. \tag{15}$$

This system can be solved using standard Monte Carlo where absorption and reemission within a timestep are approximated by an effective scatter process. Methodologies for simulating Eqs. (13) and (14) are given in Refs. [1,8].

The principal difficulty when adding electron and ion effects to this scheme is treating the conduction operator in Eqs. (10) and (11). One approach is to assume that conduction will operate at slow timescales relative to the radiation flow so that the conduction operators can be treated explicitly. This approximation will, in general, be valid because the radiation moves at the speed of light whereas the conduction is a function of the electron thermal velocity. Also, the magnitude of conduction effects is generally small compared to the coupling in high energy density physics problems. The method we develop using this approach will be called the explicit-conduction IMC (ECIMC) method.

The description of propagation of radiation based on the speed of light is not always accurate. In highly diffusive media the wave-speed that defines the radiation flow can be subsonic. In these cases we may not be able to treat the conduction explicitly. Therefore, we will have to split the system of equations such that the resulting conduction equations can be treated implicitly. We will refer to this technique as the split-conduction IMC (SCIMC) method.

Finally, we can split all of the 3T physics from the standard IMC method. In this case, we solve Eq. (13) using Monte Carlo and use (14) to get the electron energy at an intermediate time, t^{*}. We then solve split conduction and coupling equations to calculate the electron and ion internal energies at t^{n+1}. This method has the benefit that it can be easily integrated with an existing IMC code. However, this technique adds additional splits that increase the error, as we shall see in Section 4. This method will be termed the fully-split IMC (FSIMC) method.

All of the methods proposed here are written in strong conservation form. In real simulations this requires inverting the EOS at the end of each timestep to calculate the ion and electron temperatures from internal energy. This approach is consistent with hydrodynamics schemes, which include an energy equation. It also guarantees rigorous energy conservation. The drawback is the added cost of inverting tabular EOS in real calculations.

There are many additional splits that could be applied to this system. As will be shown below, the FSIMC and SCIMC methods both split the coupling such that half of the coupling is done before the conduction, and the second half is done afterward. Obviously this choice adds additional splits to these methods. We made this choice because this splitting scheme has been used in practical, radiation-hydrodynamics calculations employing diffusion for some time [4]. Also, in problems where conduction is important one would expect the accuracy to improve if the conduction and electron–ion coupling were treated simultaneously to some degree. A detailed analysis of the errors that result from different treatments of the conduction relative to the electron–ion coupling is beyond the scope of this paper.

3.1. ECIMC method

In this scheme we treat the conduction terms in Eqs. (10) and (11) explicitly; thus, we avoid the problem of inverting multiple operators during a solve. This choice makes sense as long as the timescales of the conduction terms are longer than the timescales of the radiation and coupling terms. The derivation of the method begins from the following time-discrete forms of Eqs. (9)–(11):

$$\frac{1}{c}\frac{\partial \psi}{\partial t} = -\widehat{\mathbf{\Omega}}\cdot\nabla\psi - \sigma^n\psi + \frac{1}{4\pi}\sigma^n c\phi^{n+1}; \tag{16}$$

$$\frac{e_e^{n+1}-e_e^n}{\Delta t} = \nabla\cdot D_e^n\nabla T_e^n + \frac{C_{ve}^n}{\tau^n}(T_i^{n+1}-T_e^{n+1}) + \int \sigma^n\psi\,\mathrm{d}\mathbf{\Omega} - \sigma^n c\phi^{n+1} + Q_e^n; \tag{17}$$

$$\frac{e_i^{n+1}-e_i^n}{\Delta t} = \nabla\cdot D_i^n\nabla T_i^n - \frac{C_{ve}^n}{\tau^n}(T_i^{n+1}-T_e^{n+1}) + Q_i^n. \tag{18}$$

Here, $\phi^{n+1} = a(T_e^{n+1})^4$, and we do not specify the time derivative for ψ in Eq. (16) because we will evaluate ψ piecewise-continuously during the timestep using Monte Carlo.

In order to linearize Eqs. (16)–(18), we need equations for T_e^{n+1}, T_i^{n+1}, and ϕ^{n+1}. Using the definition of $C_{v\alpha}$ in Eq. (4), we rewrite Eqs. (17) and (18) with temperature as the dependent variable:

$$C_{ve}^n\frac{T_e^{n+1}-T_e^n}{\Delta t} = \nabla\cdot D_e^n\nabla T_e^n + \frac{C_{ve}^n}{\tau^n}(T_i^{n+1}-T_e^{n+1}) + \int \sigma^n\psi\,\mathrm{d}\mathbf{\Omega} - \sigma^n c\phi^{n+1} + Q_e^n, \tag{19}$$

$$C_{vi}^n\frac{T_i^{n+1}-T_i^n}{\Delta t} = \nabla\cdot D_i^n\nabla T_i^n - \frac{C_{ve}^n}{\tau^n}(T_i^{n+1}-T_e^{n+1}) + Q_i^n. \tag{20}$$

In these equations we have chosen to evaluate C_{ve}, C_{vi}, τ, and the sources, Q_e and Q_i, at t^n. Using Eq. (20) to solve for T_i^{n+1} yields

$$T_i^{n+1} = \frac{C_{vi}^n}{\Delta t\gamma}T_i^n + \frac{C_{ve}^n}{\tau^n\gamma}T_e^{n+1} + \frac{1}{\gamma}(Q_i^n + \nabla\cdot D_i^n\nabla T_i^n), \tag{21}$$

with

$$\gamma = \frac{C_{vi}^n}{\Delta t} + \frac{C_{ve}^n}{\tau^n}. \tag{22}$$

Substituting T_i^{n+1} into Eq. (19) yields an electron equation that is decoupled from the ion equation,

$$C_{ve}^n\frac{T_e^{n+1}-T_e^n}{\Delta t} = \nabla\cdot D_e^n\nabla T_e^n + S_i^n + \alpha T_e^{n+1} + \int \sigma^n\psi\,\mathrm{d}\mathbf{\Omega} - \sigma^n c\phi^{n+1} + Q_e^n, \tag{23}$$

where

$$S_{\mathrm{i}}^{n} = \frac{C_{\mathrm{ve}}^{n}}{\tau^{n}\gamma}\left(\frac{C_{\mathrm{vi}}^{n}}{\Delta t}T_{\mathrm{i}}^{n} + Q_{\mathrm{i}}^{n} + \nabla\cdot D_{\mathrm{i}}^{n}\nabla T_{\mathrm{i}}^{n}\right), \tag{24}$$

$$\alpha = \frac{C_{\mathrm{ve}}^{n}}{\tau^{n}}\left(\frac{C_{\mathrm{ve}}^{n}}{\tau^{n}\gamma} - 1\right). \tag{25}$$

We can apply the transform shown in Eq. (12) to Eq. (17) to write an equation for the time evolution of ϕ. Using Eq. (21) to remove the ion temperature, we derive

$$\frac{1}{\beta^{n}}\frac{\phi^{n+1}-\phi^{n}}{\Delta t} = \nabla\cdot D_{\mathrm{e}}^{n}\nabla T_{\mathrm{e}}^{n} + S_{\mathrm{i}}^{n} + \alpha T_{\mathrm{e}}^{n+1} + \int \sigma^{n}\psi\,\mathrm{d}\mathbf{\Omega} - \sigma^{n}c\phi^{n+1} + Q_{\mathrm{e}}^{n}. \tag{26}$$

We have defined two equations for the time evolution of T_{e} and T_{e}^{4} in (23) and (26), respectively. Eq. (23) is used to write an expression for T_{e}^{n+1} as a function of ϕ^{n+1},

$$T_{\mathrm{e}}^{n+1} = \frac{S_{\mathrm{i}}^{n} + \frac{C_{\mathrm{ve}}^{n}}{\Delta t}T_{\mathrm{e}}^{n} + \int \sigma^{n}\psi\,\mathrm{d}\mathbf{\Omega} - \sigma^{n}c\phi^{n+1} + Q_{\mathrm{e}}^{n} + \nabla\cdot D_{\mathrm{e}}^{n}\nabla T_{\mathrm{e}}^{n}}{\frac{C_{\mathrm{ve}}^{n}}{\Delta t} - \alpha}. \tag{27}$$

Then, substituting this expression into Eq. (26), one obtains the following linear equation for ϕ^{n+1},

$$\begin{aligned}\phi^{n+1} = {} & \left[(C_{\mathrm{ve}}^{n} - \alpha\Delta t)\phi^{n} + \beta^{n}\Delta t C_{\mathrm{ve}}^{n}\times\left(\int \sigma^{n}\psi\,\mathrm{d}\mathbf{\Omega} + \nabla\cdot D_{\mathrm{e}}^{n}\nabla T_{\mathrm{e}}^{n} + S_{\mathrm{i}}^{n} + \alpha T_{\mathrm{e}}^{n} + Q_{\mathrm{e}}^{n}\right)\right] \\ & \times\left\{(1+\beta^{n}\sigma^{n}c\Delta t)C_{\mathrm{ve}}^{n} - \alpha\Delta t\right\}^{-1}.\end{aligned} \tag{28}$$

Now, we substitute ϕ^{n+1} into Eq. (16) yielding

$$\frac{1}{c}\frac{\partial\psi}{\partial t} + \hat{\mathbf{\Omega}}\cdot\nabla\psi + \sigma^{n}\psi = \frac{1}{4\pi}\left[\bar{f}\sigma^{n}c\phi^{n} + (1-\bar{f})\int \sigma^{n}\psi\,\mathrm{d}\mathbf{\Omega} + (1-\bar{f})S^{n}\right], \tag{29}$$

where we have defined the time-explicit source as

$$S^{n} = \nabla\cdot D_{\mathrm{e}}^{n}\nabla T_{\mathrm{e}}^{n} + \alpha T_{\mathrm{e}}^{n} + S_{\mathrm{i}}^{n} + Q_{\mathrm{e}}^{n}. \tag{30}$$

Here, the modified form of the standard IMC Fleck factor, $\bar{f}$, is defined

$$\bar{f} = \frac{C_{\mathrm{ve}}^{n} - \alpha\Delta t}{(1+\beta^{n}\sigma^{n}c\Delta t)C_{\mathrm{ve}}^{n} - \alpha\Delta t}. \tag{31}$$

Eq. (29) is a modified IMC transport equation that includes electron–ion coupling and conduction in the source term, S^{n}.

We can develop an electron equation that is consistent with Eq. (29) by substituting from Eqs. (21), (27), and (28), respectively, into Eq. (17). Using the definition of $\bar{f}$ we derive, after some algebraic manipulation,

$$\frac{e_{\mathrm{e}}^{n+1} - e_{\mathrm{e}}^{n}}{\Delta t} = \frac{C_{\mathrm{ve}}^{n}}{C_{\mathrm{ve}}^{n} - \alpha\Delta t}\left[\bar{f}\int \sigma^{n}\psi\,\mathrm{d}\mathbf{\Omega} - \bar{f}\sigma^{n}c\phi^{n} + \bar{f}S^{n}\right]. \tag{32}$$

Similarly, we can substitute T_{i}^{n+1}, T_{e}^{n+1}, and ϕ^{n+1} into Eq. (18) to develop a modified ion equation,

$$\frac{e_{\mathrm{i}}^{n+1} - e_{\mathrm{i}}^{n}}{\Delta t} = Q_{\mathrm{i}}^{n} + Q_{\mathrm{e}}^{n} + \nabla\cdot D_{\mathrm{e}}^{n}\nabla T_{\mathrm{e}}^{n} + \nabla\cdot D_{\mathrm{i}}^{n}\nabla T_{\mathrm{i}}^{n} - S^{n} - \frac{\alpha\Delta t}{C_{\mathrm{ve}}^{n} - \alpha\Delta t}\left[\bar{f}\int \sigma^{n}\psi\,\mathrm{d}\mathbf{\Omega} - \bar{f}\sigma^{n}c\phi^{n} + \bar{f}S^{n}\right]. \tag{33}$$

Eqs. (29), (32), and (33) can be used to solve Eqs. (16)–(18) using Monte Carlo simulation. Eq. (29) is a 3T analog of the standard IMC equation, (13), and it is solved in an identical manner. The Monte Carlo solution provides estimates of $\int \sigma^{n}\psi\,\mathrm{d}\mathbf{\Omega}$. These estimates are then used in Eqs. (32) and (33) to calculate the end-of-timestep energies and, through inversion of the EOS defined by (4), temperatures.

We note that the modified Fleck factor, $\bar{f}$, has the same limits as the standard IMC Fleck factor, $0 \leqslant \bar{f} \leqslant 1$. For $\bar{f} \geqslant 0$, $C_{\mathrm{ve}}^{n} - \alpha\Delta t$ must be greater or equal to zero because $C_{\mathrm{ve}}^{n}\beta^{n}\sigma^{n}c\Delta t > 0$. Substituting α and γ, we find that

$$\tau^{n}C_{\mathrm{vi}}^{n} + \Delta t(C_{\mathrm{ve}}^{n} + C_{\mathrm{vi}}^{n}) \geqslant 0.$$

Likewise, to show $\bar{f} \leqslant 1$ we have

$$C_{\mathrm{ve}}^n - \alpha\Delta t \leqslant (1 + \beta^n\sigma^n c\Delta t)C_{\mathrm{ve}}^n - \alpha\Delta t$$
$$C_{\mathrm{ve}}^n\beta^n\sigma^n c\Delta t \geqslant 0.$$

Because all of these terms are greater than zero, $0 \leqslant \bar{f} \leqslant 1$.

Also, when the electrons and ions are uncoupled, $\tau^n \gg 0$, and

$$\lim_{\tau^n \gg 0} \bar{f} = \frac{1}{1 + \beta^n\sigma^n c\Delta t}. \tag{34}$$

Thus, Eq. (29) limits to the standard, 2T IMC equation given in (13).

We conclude this derivation by showing that Eqs. (29), (32), and (33) are conservative. Integrating Eq. (29) over all angles (it has already been frequency integrated) yields the following balance equation,

$$\frac{\partial E}{\partial t} + \nabla \cdot \mathbf{F} = \bar{f}\sigma^n c\phi^n - \bar{f}\sigma^n cE + (1 - \bar{f})S^n, \tag{35}$$

where the radiation flux is defined

$$\mathbf{F} = \int_{4\pi} \widehat{\mathbf{\Omega}}\psi \, \mathrm{d}\mathbf{\Omega}. \tag{36}$$

Adding Eqs. (35), (32), and (33) yields

$$\frac{\partial E}{\partial t} + \frac{e_{\mathrm{e}}^{n+1} - e_{\mathrm{e}}^n}{\Delta t} + \frac{e_{\mathrm{i}}^{n+1} - e_{\mathrm{i}}^n}{\Delta t} = Q_{\mathrm{e}}^n + Q_{\mathrm{i}}^n + \nabla \cdot D_{\mathrm{e}}^n \nabla T_{\mathrm{e}}^n + \nabla \cdot D_{\mathrm{i}}^n \nabla T_{\mathrm{i}}^n - \nabla \cdot \mathbf{F}. \tag{37}$$

This equation is a correct balance equation that states that the change in the total energy in the system is equal to the sources minus the amount of energy flow through the system.

3.2. SCIMC method

In this method the conduction operator is split from the electron and ion equations. The resulting system has three splits. Split **I** includes half of the electron–ion coupling and solves for the end-of-timestep radiation intensity and the electron and ion energies at t':

$$\frac{1}{c}\frac{\partial \psi}{\partial t} = -\widehat{\mathbf{\Omega}} \cdot \nabla\psi - \sigma^n\psi + \frac{1}{4\pi}\sigma^n c\phi'; \tag{38}$$

$$\frac{e_{\mathrm{e}}' - e_{\mathrm{e}}^n}{\Delta t} = \frac{C_{\mathrm{ve}}^n}{2\tau^n}(T_{\mathrm{i}}' - T_{\mathrm{e}}') + \int \sigma^n\psi \, \mathrm{d}\mathbf{\Omega} - \sigma^n c\phi' + Q_{\mathrm{e}}^n; \tag{39}$$

$$\frac{e_{\mathrm{i}}' - e_{\mathrm{i}}^n}{\Delta t} = -\frac{C_{\mathrm{ve}}^n}{2\tau^n}(T_{\mathrm{i}}' - T_{\mathrm{e}}') + Q_{\mathrm{i}}^n. \tag{40}$$

Split **II** solves the conduction equations to get the energies at t'':

$$\frac{e_{\mathrm{e}}'' - e_{\mathrm{e}}'}{\Delta t} = \nabla \cdot D_{\mathrm{e}}\nabla T_{\mathrm{e}}''; \tag{41}$$

$$\frac{e_{\mathrm{i}}'' - e_{\mathrm{i}}'}{\Delta t} = \nabla \cdot D_{\mathrm{i}}\nabla T_{\mathrm{i}}''. \tag{42}$$

The final split, **III**, solves the second half of the electron–ion coupling using equations:

$$\frac{e_{\mathrm{e}}^{n+1} - e_{\mathrm{e}}''}{\Delta t} = \frac{C_{\mathrm{ve}}}{2\tau}(T_{\mathrm{i}}^{n+1} - T_{\mathrm{e}}^{n+1}); \tag{43}$$

$$\frac{e_{\mathrm{i}}^{n+1} - e_{\mathrm{i}}''}{\Delta t} = -\frac{C_{\mathrm{ve}}}{2\tau}(T_{\mathrm{i}}^{n+1} - T_{\mathrm{e}}^{n+1}). \tag{44}$$

Note that in splits **II** and **III** we do not specify the time-level of the coefficients D_{e}, D_{i}, C_{ve}, and τ. These splits can be solved nonlinearly using Newton's method or by linearizing through Eq. (4). We will show results from both calculations in Section 6.4.

Splits **II** and **III** were selected in order to preserve the physical coupling between conduction and the electron–ion coupling. In practice one could solve the conduction equations before or after the complete electron–ion coupling. This choice is reasonable; however, it neglects the impact that the electron–ion coupling has on the conduction.

We can formulate a Monte Carlo method to solve split **I**. The derivation of the equations is analogous to the procedure used for the ECIMC method in Section 3.1. The resulting system of modified IMC equations that solves **I** is

$$\frac{1}{c}\frac{\partial \psi}{\partial t} + \widehat{\mathbf{\Omega}} \cdot \nabla \psi + \sigma^n \psi = \frac{1}{4\pi}\left[\hat{f}\sigma^n c\phi^n + (1-\hat{f})\int \sigma^n \psi \, \mathrm{d}\mathbf{\Omega} + (1-\hat{f})\hat{S}^n\right], \tag{45}$$

$$\frac{e'_\mathrm{e} - e^n_\mathrm{e}}{\Delta t} = \frac{C^n_\mathrm{ve}}{C^n_\mathrm{ve} - \hat{\alpha}\Delta t}\left[\hat{f}\int \sigma^n \psi \, \mathrm{d}\mathbf{\Omega} - \hat{f}\sigma^n c\phi^n + \hat{f}\hat{S}^n\right], \tag{46}$$

$$\frac{e'_\mathrm{i} - e^n_\mathrm{i}}{\Delta t} = Q^n_\mathrm{i} + Q^n_\mathrm{e} - \hat{S}^n - \frac{\hat{\alpha}\Delta t}{C^n_\mathrm{ve} - \hat{\alpha}\Delta t}\left[\hat{f}\int \sigma^n \psi \, \mathrm{d}\mathbf{\Omega} - \hat{f}\sigma^n c\phi^n + \hat{f}\hat{S}^n\right]. \tag{47}$$

These equations are identical in form to Eqs. (29), (32), and (33). The differences lie in the modified source term $\widehat{S}^n$, coefficient $\hat{\alpha}$, and Fleck factor $\hat{f}$ that are defined by

$$\widehat{S}^n = \hat{\alpha}T^n_\mathrm{e} + \widehat{S}^n_\mathrm{i} + Q^n_\mathrm{e}, \tag{48}$$

$$\hat{\alpha} = \frac{C^n_\mathrm{ve}}{2\tau^n}\left(\frac{C^n_\mathrm{ve}}{2\tau^n\hat{\gamma}} - 1\right), \tag{49}$$

$$\hat{f} = \frac{C^n_\mathrm{ve} - \hat{\alpha}\Delta t}{(1+\beta^n\sigma^n c\Delta t)C^n_\mathrm{ve} - \hat{\alpha}\Delta t}. \tag{50}$$

The explicit ion source term, $\widehat{S}^n_\mathrm{i}$, and $\hat{\gamma}$ are defined,

$$\widehat{S}^n_\mathrm{i} = \frac{C^n_\mathrm{ve}}{2\tau^n\hat{\gamma}}\left(\frac{C^n_\mathrm{vi}}{\Delta t}T^n_\mathrm{i} + Q^n_\mathrm{i}\right), \tag{51}$$

$$\hat{\gamma} = \frac{C^n_\mathrm{vi}}{\Delta t} + \frac{C^n_\mathrm{ve}}{2\tau^n}. \tag{52}$$

Also, Eq. (47) has no conduction terms because these have been split off.

Eqs. (45)–(47) can be used to solve Eqs. (38)–(40) using Monte Carlo simulation. We simulate Eq. (38) with Monte Carlo in the same way as Eq. (29). Eqs. (39) and (40) are solved to get the energies at t'. Splits **II** and **III** are then solved to get the final energies and temperatures at t^{n+1}.

This method will be more robust than the ECIMC scheme at large timesteps when the conduction timescales are the same order as the radiation timescales. However, the SCIMC method requires two additional implicit solves for the conduction equations. When the second half of the coupling equations are linearized, it requires a sweep of the mesh to solve split **III**. Alternatively, block-Newton iterations can be used; however, these are more expensive. Also, the additional splits in this scheme impose errors that are not present in ECIMC as we will show in Section 4.

3.3. FSIMC method

The final 3T Monte Carlo method we will consider is a fully-split scheme. Here, we use standard IMC, see Eqs. (13) and (14), to solve for the radiation intensity and electron energy at t^*. The rest of the coupling terms are split and can be solved after the Monte Carlo transport simulation. Effectively, this method is similar to the SCIMC scheme except we add an additional split to **I**. Thus, we define split **Ia**:

$$\frac{1}{c}\frac{\partial \psi}{\partial t} = -\widehat{\mathbf{\Omega}} \cdot \nabla \psi - \sigma^n \psi + \frac{1}{4\pi}\sigma^n c\phi^*; \tag{53}$$

$$\frac{e^*_\mathrm{e} - e^n_\mathrm{e}}{\Delta t} = \int \sigma^n \psi \, \mathrm{d}\mathbf{\Omega} - \sigma^n c\phi^* + Q^n_\mathrm{e}. \tag{54}$$

The equations in **Ia** are identical to the 2T equations that are used to formulate the standard IMC method. Split **Ib** adds half of the electron–ion coupling and the ion source:

$$\frac{e'_{\mathrm{e}} - e^*_{\mathrm{e}}}{\Delta t} = \frac{C^n_{\mathrm{ve}}}{2\tau^n}(T'_{\mathrm{i}} - T'_{\mathrm{e}}); \tag{55}$$

$$\frac{e'_{\mathrm{i}} - e^n_{\mathrm{i}}}{\Delta t} = -\frac{C^n_{\mathrm{ve}}}{2\tau^n}(T'_{\mathrm{i}} - T'_{\mathrm{e}}) + Q^n_{\mathrm{i}}. \tag{56}$$

The next two splits are identical to Eqs. (41), (42) (split **II**) and Eqs. (43), (44) (split **III**) from the SCIMC method.

Split **Ia** is solved with standard IMC using Eqs. (13) and (14). Eq. (14) is integrated from e^*_{e} to e^n_{e}, and the source term is simply the electron source, $Q^n \equiv Q^n_{\mathrm{e}}$. For the FSIMC method, $T \equiv T_{\mathrm{e}}$ in Eqs. (13) and (14).

The principal advantage of the FSIMC method is that it it easily integrated with an existing IMC implementation. Also, it can be used in problems where the conduction timescales are equivalent to the radiation timescales. Like the SCIMC scheme, this method requires additional solves for the ion–electron conduction and coupling equations. It also requires one additional sweep of the mesh to solve for the electron energy at t^*. As in SCIMC, FSIMC adds additional error due to the extra splits in the method when compared to ECIMC. These errors will be shown in Section 4.

4. Modified equation analysis

Modified equation analysis (MEA) is a useful technique for analyzing time-integration errors that result from operator splits and linearization. In short, MEA uses Taylor series expansions to bring all variables and state vectors to the advanced time level for a system of equations. The procedure employed here follows closely the analysis shown in Ref. [7]. A formal mathematical description of the technique can be found in Ref. [6].

We will apply MEA to the three IMC schemes that have been proposed to solve Eqs. (9)–(11). For simplicity, we will only consider infinite medium solutions. Additionally, we will make the assumption that C_{ve}, C_{vi} and τ are constant. In this case, the material energy is directly related to the temperature through the EOS relationship,

$$e_\alpha = \int_0^T C_{\mathrm{v}\alpha}\,\mathrm{d}T'_\alpha = C_{\mathrm{v}\alpha}T_\alpha, \tag{57}$$

where $\alpha = \mathrm{e}, \mathrm{i}$ for electrons and ions. Using these assumptions, if we ignore the spatial terms in Eqs. (9)–(11) and integrate the transport equation over angle, we have

$$\frac{\partial E}{\partial t} + \sigma c E = \sigma c \phi, \tag{58a}$$

$$C_{\mathrm{ve}}\frac{\partial T_{\mathrm{e}}}{\partial t} = \frac{C_{\mathrm{ve}}}{\tau}(T_{\mathrm{i}} - T_{\mathrm{e}}) + \sigma c E - \sigma c \phi, \tag{58b}$$

$$C_{\mathrm{vi}}\frac{\partial T_{\mathrm{i}}}{\partial t} = -\frac{C_{\mathrm{ve}}}{\tau}(T_{\mathrm{i}} - T_{\mathrm{e}}) + Q_{\mathrm{i}}. \tag{58c}$$

Note that $Q_{\mathrm{e}} = 0$ in this analysis. Eq. (58) are not written in strong conservation form, and the principal unknowns are E, T_{e}, and T_{i}.

By ignoring space dependence in Eqs. (58b), (58c) we neglect to account for conduction effects on the splitting and linearization errors. However, including space-dependence and conduction presents several difficulties. First, MEA requires nonlinear-consistent solutions of the modified equations, and we have no good methods for performing fully nonlinear Monte Carlo calculations. We could employ a deterministic technique to generate MEA solutions, but nonlinear-consistent, deterministic transport methods are still an active area of research. Also, conduction is often a small effect for high energy density physics applications. For example, ion conduction is not even considered in the multi-T fluid approximations used in Ref. [9]. Thus, our analysis focuses on the errors associated with splitting the ion–electron coupling terms and linearizing the transport and electron equations.

When conduction can be neglected in a particular problem, the ECIMC method is the preferred option. The ECIMC method absent conduction is derived by removing the $\nabla \cdot D\nabla T$ terms from Eqs. (24), (30), and (33). This method has no splits in the radiation solution, and it will be more accurate than simulating the standard IMC equations followed by an electron–ion coupling solve. In the analysis that follows we will consider the SCIMC and FSIMC methods with the splits that bound the conduction solve, even though the conduction splits are not present in the simplified equations. The analysis will show the errors that result from splitting the electron–ion coupling if conduction were present.

In order to illustrate the MEA procedure, we show the full derivation of the modified equations for the SCIMC method. Afterward, we will simply write down the modified equations for the ECIMC and FSIMC schemes. All of the MEA will be applied to the simplified system in Eqs. (58a)–(58c).

4.1. Modified SCIMC equations

In analogy to the space-dependent system described in Section 3.2, the SCIMC method is derived from the following operator-split and discretized form of Eqs. (58a)–(58c):

$$\frac{\partial E}{\partial t} = \sigma^n c(\phi' - E); \tag{59}$$

$$C_{\mathrm{ve}}\frac{T'_{\mathrm{e}} - T^n_{\mathrm{e}}}{\Delta t} = \frac{C_{\mathrm{ve}}}{2\tau}(T'_{\mathrm{i}} - T'_{\mathrm{e}}) + \sigma^n c(E - \phi'); \tag{60}$$

$$C_{\mathrm{vi}}\frac{T'_{\mathrm{i}} - T^n_{\mathrm{i}}}{\Delta t} = -\frac{C_{\mathrm{ve}}}{2\tau}(T'_{\mathrm{i}} - T'_{\mathrm{e}}) + Q^n_{\mathrm{i}}; \tag{61}$$

$$\frac{1}{\beta^n}\frac{\phi' - \phi^n}{\Delta t} = \frac{C_{\mathrm{ve}}}{2\tau}(T'_{\mathrm{i}} - T'_{\mathrm{e}}) + \sigma^n c(E - \phi'); \tag{62}$$

$$C_{\mathrm{ve}}\frac{T_{\mathrm{e}} - T'_{\mathrm{e}}}{\Delta t} = \frac{C_{\mathrm{ve}}}{2\tau}(T_{\mathrm{i}} - T_{\mathrm{e}}); \tag{63}$$

$$C_{\mathrm{vi}}\frac{T_{\mathrm{i}} - T'_{\mathrm{i}}}{\Delta t} = -\frac{C_{\mathrm{ve}}}{2\tau}(T_{\mathrm{i}} - T_{\mathrm{e}}). \tag{64}$$

Here, and in what follows, E, T_{e}, T_{i}, and ϕ written without superscripts indicates a quantity that is evaluated at t^{n+1}. The simplified SCIMC method that results from these equations is

$$\frac{\partial E}{\partial t} + \hat{f}\sigma^n cE = \hat{f}\sigma^n c\phi^n + (1 - \hat{f})\widehat{S}^n, \tag{65a}$$

$$C_{\mathrm{ve}}\frac{T'_{\mathrm{e}} - T^n_{\mathrm{e}}}{\Delta t} = \frac{C_{\mathrm{ve}}}{C_{\mathrm{ve}} - \alpha\Delta t}(\hat{f}\sigma^n cE - \hat{f}\sigma^n c\phi^n + \hat{f}\widehat{S}^n), \tag{65b}$$

$$C_{\mathrm{vi}}\frac{T'_{\mathrm{i}} - T^n_{\mathrm{i}}}{\Delta t} = Q^n_{\mathrm{i}} - \widehat{S}^n - \frac{\alpha\Delta t}{C_{\mathrm{ve}} - \alpha\Delta t}(\hat{f}\sigma^n cE - \hat{f}\sigma^n c\phi^n + \hat{f}\widehat{S}^n), \tag{65c}$$

$$C_{\mathrm{ve}}\frac{T_{\mathrm{e}} - T'_{\mathrm{e}}}{\Delta t} = \frac{C_{\mathrm{ve}}C_{\mathrm{vi}}}{2\tau C_{\mathrm{vi}} + \Delta t(C_{\mathrm{vi}} + C_{\mathrm{ve}})}(T'_{\mathrm{i}} - T'_{\mathrm{e}}), \tag{65d}$$

$$C_{\mathrm{vi}}\frac{T_{\mathrm{i}} - T'_{\mathrm{i}}}{\Delta t} = \frac{-C_{\mathrm{ve}}C_{\mathrm{vi}}}{2\tau C_{\mathrm{vi}} + \Delta t(C_{\mathrm{vi}} + C_{\mathrm{ve}})}(T'_{\mathrm{i}} - T'_{\mathrm{e}}). \tag{65e}$$

The first three equations are the simplified analog to Eqs. (45)–(47). The last two equations solve Eqs. (43), (44). Because C_{ve}, C_{vi}, and τ are constant, the second half of the ion–electron coupling is linear and can be solved by direct substitution.

The SCIMC equations are derived from Eqs. (59)–(64). In order to form modified equations we need to bring all state vectors and variables to the advanced time level, t^{n+1}. This is achieved via the following Taylor-series expansion,

$$g^n = g - \Delta t\dot{g} + \frac{\Delta t^2}{2}\ddot{g} + \mathrm{O}(\Delta t^3), \tag{66}$$

where $g \equiv g^{n+1}$ and $\dot{g}$ and $\ddot{g}$ indicate first and second derivatives with respect to t, respectively. Now, consider the transport equation in (59) with first-order differencing applied to the time derivative. In a Monte Carlo simulation we actually do a piecewise-continuous solve of E; however, for the purposes of this analysis we will consider a first-order solution to E. If we expand all of the t^n terms we get the following equation,

$$\frac{1}{\Delta t}\left(E - E + \Delta t\dot{E} - \frac{\Delta t^2}{2}\ddot{E}\right) + \left(\sigma - \Delta t\dot{\sigma} + \frac{\Delta t^2}{2}\ddot{\sigma}\right)(cE - c\phi') + \mathrm{O}(\Delta t^3) = 0. \tag{67}$$

Here we have a problem because ϕ' is defined at t'. However, we can transform Eq. (63) to find an expression for ϕ',

$$\frac{1}{\beta^n}\frac{\phi - \phi'}{\Delta t} = \frac{C_{\mathrm{ve}}}{2\tau}(T_{\mathrm{i}} - T_{\mathrm{e}}). \tag{68}$$

Solving for ϕ' and expanding β^n we get

$$\phi' = \phi - \Delta t\beta\frac{C_{\mathrm{ve}}}{2\tau}(T_{\mathrm{i}} - T_{\mathrm{e}}) + \Delta t^2\dot{\beta}\frac{C_{\mathrm{ve}}}{2\tau}(T_{\mathrm{i}} - T_{\mathrm{e}}) + \mathrm{O}(\Delta t^3). \tag{69}$$

Substituting ϕ' into Eq. (67) and moving all first-order terms to the right-hand side, we get the following modified equation for E,

$$\dot{E} + \sigma c(E - \phi) = \frac{\Delta t}{2}\ddot{E} + \Delta t\dot{\sigma}c(E - \phi) - \Delta t\sigma c\beta\frac{C_{\mathrm{ve}}}{2\tau}(T_{\mathrm{i}} - T_{\mathrm{e}}) + \mathrm{O}(\Delta t^2). \tag{70}$$

Analysis of the left-hand side of Eq. (70) shows that it is identical to Eq. (58a). The right-hand side gives the first-order errors imposed by the linearization and splitting that we have used to solve Eqs. (58a)–(58c).

Continuing with our analysis, we now add Eqs. (60) and (63) and Eqs. (61) and (64) yielding

$$C_{\mathrm{ve}}\frac{T_{\mathrm{e}} - T_{\mathrm{e}}^n}{\Delta t} = \frac{C_{\mathrm{ve}}}{2\tau}(T_{\mathrm{i}} - T_{\mathrm{e}}) + \frac{C_{\mathrm{ve}}}{2\tau}(T'_{\mathrm{i}} - T'_{\mathrm{e}}) + \sigma^n c(E - \phi'), \tag{71}$$

$$C_{\mathrm{vi}}\frac{T_{\mathrm{i}} - T_{\mathrm{i}}^n}{\Delta t} = -\frac{C_{\mathrm{ve}}}{2\tau}(T_{\mathrm{i}} - T_{\mathrm{e}}) - \frac{C_{\mathrm{ve}}}{2\tau}(T'_{\mathrm{i}} - T'_{\mathrm{e}}) + Q_{\mathrm{i}}^n. \tag{72}$$

In order to form modified equations, we need to define T'_{i} and T'_{e}. We use Eqs. (63) and (64) to write functions for T'_{i} and T'_{e} evaluated at t^{n+1} as follows,

$$T'_{\mathrm{e}} = T_{\mathrm{e}} - \frac{\Delta t}{2\tau}(T_{\mathrm{i}} - T_{\mathrm{e}}), \tag{73}$$

$$T'_{\mathrm{i}} = T_{\mathrm{i}} + \frac{\Delta t}{2\tau}\frac{C_{\mathrm{ve}}}{C_{\mathrm{vi}}}(T_{\mathrm{i}} - T_{\mathrm{e}}). \tag{74}$$

Using Eqs. (69), (73), and (74) for ϕ', T'_{e}, and T'_{i} in Eqs. (71) and (72) and expanding t^n quantities to include first-order terms and moving all first-order terms to the right-hand side, we get the following modified equations for the electron temperature,

$$\begin{aligned} C_{\mathrm{ve}}\dot{T}_{\mathrm{e}} - \frac{C_{\mathrm{ve}}}{\tau}(T_{\mathrm{i}} - T_{\mathrm{e}}) + \sigma c(\phi - E) = {} & \frac{\Delta t}{2}C_{\mathrm{ve}}\ddot{T}_{\mathrm{e}} + \Delta t\dot{\sigma}c(\phi - E) + \Delta t\frac{C_{\mathrm{ve}}}{4\tau^2}\left(\frac{C_{\mathrm{ve}}}{C_{\mathrm{vi}}} + 1\right)(T_{\mathrm{i}} - T_{\mathrm{e}}) \\ & + \Delta t\sigma c\beta\frac{C_{\mathrm{ve}}}{2\tau}(T_{\mathrm{i}} - T_{\mathrm{e}}) + \mathrm{O}(\Delta t^2), \end{aligned} \tag{75}$$

and ion temperature,

$$C_{\mathrm{vi}}\dot{T}_{\mathrm{i}} + \frac{C_{\mathrm{ve}}}{\tau}(T_{\mathrm{i}} - T_{\mathrm{e}}) - Q_{\mathrm{i}} = \frac{\Delta t}{2}C_{\mathrm{vi}}\ddot{T}_{\mathrm{i}} - \Delta t\dot{Q}_{\mathrm{i}} - \Delta t\frac{C_{\mathrm{ve}}}{4\tau^2}\left(\frac{C_{\mathrm{ve}}}{C_{\mathrm{vi}}} + 1\right)(T_{\mathrm{i}} - T_{\mathrm{e}}) + \mathrm{O}(\Delta t^2). \tag{76}$$

The left-hand sides of Eqs. (75) and (76) are identical to Eqs. (58b) and (58c). As in the case of Eq. (70) the terms on the right-hand sides of Eqs. (75) and (76) are the errors that result from the linearization and splitting strategy employed in the SCIMC method.

Eqs. (70), (75), and (76) are modified equations that show the errors that result from solving (58a)–(58c) using Eqs. (65a)–(65e). However, the linearization strategy employed in IMC methods uses an additional equation that describes the time evolution of ϕ. These effects must be included in order to accurately account for all of the errors. We substitute Eqs. (69), (73), and (74) into Eq. (62) and expand the t_n quantities. Keeping all first-order terms and rearranging by moving all $O(\Delta t)$ terms to the right-hand side, we obtain the following modified equation for ϕ,

$$\frac{1}{\beta}\dot{\phi} - \frac{C_{ve}}{\tau}(T_i - T_e) + \sigma c(\phi - E) = \frac{\Delta t}{2}\frac{1}{\beta}\ddot{\phi} + \Delta t\dot{\sigma}c(\phi - E) + \Delta t\frac{C_{ve}}{4\tau^2}\left(\frac{C_{ve}}{C_{vi}} + 1\right)(T_i - T_e) + \Delta t\sigma c\beta\frac{C_{ve}}{2\tau} \times (T_i - T_e) - \Delta t\frac{\dot{\beta}}{\beta}\frac{C_{ve}}{\tau}(T_i - T_e) + \Delta t\frac{\dot{\beta}}{\beta}\sigma c(\phi - E) + O(\Delta t^2). \tag{77}$$

This equation has no direct analog in Eqs. (58a)–(58c); however, it does give the error that results from using Eq. (62) to linearize the T_e^4 terms in Eqs. (59) and (60).

4.2. Modified ECIMC and FSIMC equations

Following an analogous process to that described in Section 4.1, we can develop modified equations for both the ECIMC and FSIMC methods. The modified equations for the ECIMC scheme are:

$$\dot{E} + \sigma c(E - \phi) = \frac{\Delta t}{2}\ddot{E} + \Delta t\dot{\sigma}c(E - \phi) + O(\Delta t^2); \tag{78}$$

$$C_{ve}\dot{T}_e - \frac{C_{ve}}{\tau}(T_i - T_e) + \sigma c(\phi - E) = \frac{\Delta t}{2}C_{ve}\ddot{T}_e + \Delta t\dot{\sigma}c(\phi - E) + O(\Delta t^2); \tag{79}$$

$$C_{vi}\dot{T}_i + \frac{C_{ve}}{\tau}(T_i - T_e) - Q_i = \frac{\Delta t}{2}C_{vi}\ddot{T}_i - \Delta t\dot{Q}_i + O(\Delta t^2); \tag{80}$$

$$\frac{1}{\beta}\dot{\phi} - \frac{C_{ve}}{\tau}(T_i - T_e) + \sigma c(\phi - E) = \frac{\Delta t}{2}\frac{1}{\beta}\ddot{\phi} + \Delta t\dot{\sigma}c(\phi - E) - \Delta t\frac{\dot{\beta}}{\beta}\frac{C_{ve}}{\tau}(T_i - T_e) + \Delta t\frac{\dot{\beta}}{\beta}\sigma c(\phi - E) + O(\Delta t^2). \tag{81}$$

Similarly, the modified equations for the FSIMC scheme are:

$$\dot{E} + \sigma c(E - \phi) = \frac{\Delta t}{2}\ddot{E} + \Delta t\dot{\sigma}c(E - \phi) - \Delta t\sigma c\beta\frac{C_{ve}}{\tau}(T_i - T_e) + O(\Delta t^2); \tag{82}$$

$$C_{ve}\dot{T}_e - \frac{C_{ve}}{\tau}(T_i - T_e) + \sigma c(\phi - E) = \frac{\Delta t}{2}C_{ve}\ddot{T}_e + \Delta t\dot{\sigma}c(\phi - E) + \Delta t\frac{C_{ve}}{4\tau^2}\left(\frac{C_{ve}}{C_{vi}} + 1\right)(T_i - T_e) + \Delta t\sigma c\beta\frac{C_{ve}}{\tau}(T_i - T_e) + O(\Delta t^2); \tag{83}$$

$$C_{vi}\dot{T}_i + \frac{C_{ve}}{\tau}(T_i - T_e) - Q_i = \frac{\Delta t}{2}C_{vi}\ddot{T}_i - \Delta t\dot{Q}_i - \Delta t\frac{C_{ve}}{4\tau^2}\left(\frac{C_{ve}}{C_{vi}} + 1\right)(T_i - T_e) + O(\Delta t^2); \tag{84}$$

$$\frac{1}{\beta}\dot{\phi} - \frac{C_{ve}}{\tau}(T_i - T_e) + \sigma c(\phi - E) = \frac{\Delta t}{2}\frac{1}{\beta}\ddot{\phi} + \Delta t\dot{\sigma}c(\phi - E) + \Delta t\frac{C_{ve}}{4\tau^2}\left(\frac{C_{ve}}{C_{vi}} + 1\right)(T_i - T_e) + \Delta t\sigma c\beta\frac{C_{ve}}{\tau}(T_i - T_e) - \Delta t\frac{\dot{\beta}}{\beta}\frac{C_{ve}}{\tau}(T_i - T_e) + \Delta t\frac{\dot{\beta}}{\beta}\sigma c(\phi - E) + O(\Delta t^2). \tag{85}$$

The only difference between the SCIMC and FSIMC modified equations is in the following error term,

$$\underbrace{\Delta t\sigma c\beta\frac{C_{ve}}{2\tau}(T_i - T_e)}_{\text{SCIMC}} \rightarrow \underbrace{\Delta t\sigma c\beta\frac{C_{ve}}{\tau}(T_i - T_e)}_{\text{FSIMC}}. \tag{86}$$

Hence, this term is twice as large when using the FSIMC method. We shall examine its impact in Section 5.

At this point, one could inquire about variants of the FSIMC method when electron–ion conduction is not required for a given problem. In that case, an alternative form of the FSIMC method could be derived that

splits the electron–ion coupling from the IMC in a single step. MEA analysis of this system shows that the errors are identical to the ECIMC method except that the $\Delta t\sigma c\beta\frac{C_{ve}}{\tau}(T_i - T_e)$ term is present in the alternate FSIMC scheme. This term, as we shall show in Section 5, represents a source of unbounded error, and therefore, the ECIMC method will be the most accurate scheme when conduction is neglected.

5. MEA computational results

We can use the modified equations derived in Section 4 to estimate the errors that result from the various linearization and splitting schemes that we employ in our IMC methods. The error terms are estimated by solving the modified equations with fully resolved nonlinearities. In this study, Newton's method is used to generate nonlinear solutions to the modified equations.

To begin, we write the system of modified equations with first-order differencing,

$$\frac{E - E^n}{\Delta t} + \sigma c(E - \phi) = \xi_1, \tag{87a}$$

$$C_{ve}\frac{T_e - T_e^n}{\Delta t} - \frac{C_{ve}}{\tau}(T_i - T_e) + \sigma c(\phi - E) = \xi_2, \tag{87b}$$

$$C_{vi}\frac{T_i - T_i^n}{\Delta t} + \frac{C_{ve}}{\tau}(T_i - T_e) - Q_i = \xi_3, \tag{87c}$$

with ϕ defined (see Eqs. (77), (81), and (85))

$$\phi = \frac{\xi_4 + \phi^n + \beta\Delta t\frac{C_{ve}}{\tau}(T_i - T_e) + \beta\sigma c\Delta t E}{1 + \beta\sigma c\Delta t}. \tag{88}$$

The error terms, $\{\xi_1, \xi_2, \xi_3, \xi_4\}$, are unique to the IMC method for which the modified equations are defined. The first-order differencing scheme allows us to ignore the $\ddot{E}$, $\ddot{T}_e$, $\ddot{T}_i$, and $\ddot{\phi}$ error terms because they are identical to the errors imposed by numerically solving the equations to first order. Additionally, we evaluate $\dot{\sigma}$ and $\dot{\beta}$ to first order. Using these approximations, the error terms (ξ) for each IMC method are defined:

ECIMC:

$$\xi_1 = c\frac{\partial\sigma}{\partial T_e}(T_e - T_e^n)(E - \phi); \tag{89a}$$

$$\xi_2 = c\frac{\partial\sigma}{\partial T_e}(T_e - T_e^n)(\phi - E); \tag{89b}$$

$$\xi_3 = -\Delta t\dot{Q}_i; \tag{89c}$$

$$\xi_4 = c\frac{\partial\sigma}{\partial T_e}(T_e - T_e^n)(\phi - E) - \frac{1}{\beta}\frac{C_{ve}}{\tau}\frac{\partial\beta}{\partial T_e}(T_e - T_e^n)(T_i - T_e) + \frac{1}{\beta}\frac{\partial\beta}{\partial T_e}\sigma c(T_e - T_e^n)(\phi - E); \tag{89d}$$

SCIMC:

$$\xi_1 = c\frac{\partial\sigma}{\partial T_e}(T_e - T_e^n)(E - \phi) - \Delta t\sigma c\beta\frac{C_{ve}}{2\tau}(T_i - T_e); \tag{90a}$$

$$\xi_2 = c\frac{\partial\sigma}{\partial T_e}(T_e - T_e^n)(\phi - E) + \Delta t\frac{C_{ve}}{4\tau^2}\left(\frac{C_{ve}}{C_{vi}} + 1\right)(T_i - T_e) + \Delta t\sigma c\beta\frac{C_{ve}}{2\tau}(T_i - T_e); \tag{90b}$$

$$\xi_3 = -\Delta t\dot{Q}_i - \Delta t\frac{C_{ve}}{4\tau^2}\left(\frac{C_{ve}}{C_{vi}} + 1\right)(T_i - T_e); \tag{90c}$$

$$\xi_4 = c\frac{\partial\sigma}{\partial T_e}(T_e - T_e^n)(\phi - E) + \Delta t\frac{C_{ve}}{4\tau^2}\left(\frac{C_{ve}}{C_{vi}} + 1\right)(T_i - T_e) + \Delta t\sigma c\beta\frac{C_{ve}}{2\tau}(T_i - T_e) - \frac{1}{\beta}\frac{C_{ve}}{\tau}\frac{\partial\beta}{\partial T_e}(T_e - T_e^n)(T_i - T_e) + \frac{1}{\beta}\frac{\partial\beta}{\partial T_e}\sigma c(T_e - T_e^n)(\phi - E); \tag{90d}$$

FSIMC:

$$\xi_1 = c\frac{\partial\sigma}{\partial T_e}(T_e - T_e^n)(E-\phi) - \Delta t\sigma c\beta\frac{C_{ve}}{\tau}(T_i - T_e); \tag{91a}$$

$$\xi_2 = c\frac{\partial\sigma}{\partial T_e}(T_e - T_e^n)(\phi-E) + \Delta t\frac{C_{ve}}{4\tau^2}\left(\frac{C_{ve}}{C_{vi}}+1\right)(T_i - T_e) + \Delta t\sigma c\beta\frac{C_{ve}}{\tau}(T_i - T_e); \tag{91b}$$

$$\xi_3 = -\Delta t\dot{Q}_i - \Delta t\frac{C_{ve}}{4\tau^2}\left(\frac{C_{ve}}{C_{vi}}+1\right)(T_i - T_e); \tag{91c}$$

$$\xi_4 = c\frac{\partial\sigma}{\partial T_e}(T_e - T_e^n)(\phi-E) + \Delta t\frac{C_{ve}}{4\tau^2}\left(\frac{C_{ve}}{C_{vi}}+1\right)(T_i - T_e) + \Delta t\sigma c\beta\frac{C_{ve}}{\tau}(T_i - T_e) - \frac{1}{\beta}\frac{C_{ve}}{\tau}\frac{\partial\beta}{\partial T_e}(T_e - T_e^n)(T_i - T_e) + \frac{1}{\beta}\frac{\partial\beta}{\partial T_e}\sigma c(T_e - T_e^n)(\phi - E). \tag{91d}$$

These equations constitute the discrete forms of the modified equations for each IMC method defined for the simplified system in Eqs. (58a)–(58c).

Solving the modified equations should reproduce, minus high-order terms, the solutions obtained using the appropriate split, linearized method. If modified equations with second-order, or higher, error terms are required to reproduce the results from the IMC solutions, the method will not be first-order convergent. For example, if we solve Eqs. (87a)–(87c) with error terms defined by Eqs. (90a)–(90d) using a fully nonlinear method, the solution should reproduce the results obtained by solving Eqs. (65a)–(65e).

5.1. Model problem

We consider a problem that starts with radiation, electrons, and ions at room temperature (293 K). We apply a Gaussian-fitted source to the ions using

$$Q_i(t) = \rho\mathfrak{C}\frac{\exp\left(\frac{(t-t_c)^2}{2t_w^2}\right)}{\sqrt{2\pi}t_w}\ [\text{GJ cm}^{-3}\ \text{ns}^{-1}], \tag{92}$$

where $\mathfrak{C}$ is a normalization constant and t_w is the width of the source. The source is centered about t_c.

The model problem has the following data:

$$\mathfrak{C} = 25.06628, \quad t_w = 1.0\ \text{ns}, \quad t_c = 10.0\ \text{ns}$$

$$\sigma = \frac{\sigma_0}{T_e^2}\ \text{cm}^{-1}, \quad \frac{\partial\sigma}{\partial T_e} = -\frac{2\sigma_0}{T_e^3}, \quad \sigma_0 = 0.5$$

$$C_{ve} = 0.1\rho, \quad C_{vi} = 0.05\rho\ [\text{GJ cm}^{-3}\ \text{keV}^{-1}]$$

$$\tau = 0.1\ \text{ns}$$

$$\rho = 3.0\ \text{g cm}^{-3}$$

The initial conditions are

$$T_i(0) = T_e(0) = T_r(0) = T_0 = 293\ ^\circ\text{K} = 2.52487\times10^{-5}\ \text{keV}$$

$$E(0) = 5.57585\times10^{-21}\ \text{GJ cm}^{-3}$$

$$e_e(0) = 7.57461\times10^{-6}\ \text{GJ cm}^{-3}$$

$$e_i(0) = 3.78731\times10^{-6}\ \text{GJ cm}^{-3}$$

Second-order benchmark solutions for this problem are calculated using Crank–Nicolson differencing with nonlinear Newton iteration and timesteps of 10^{-5} ns.

A comparison of results from each IMC method with the benchmark solution to the model problem is shown in Fig. 1. The ECIMC method is the most accurate, followed by SCIMC. Using the MEA solutions in Eqs. (87)–(91) we can quantify the errors that hamper the accuracy of the SCIMC and FSIMC methods relative to the ECIMC method.

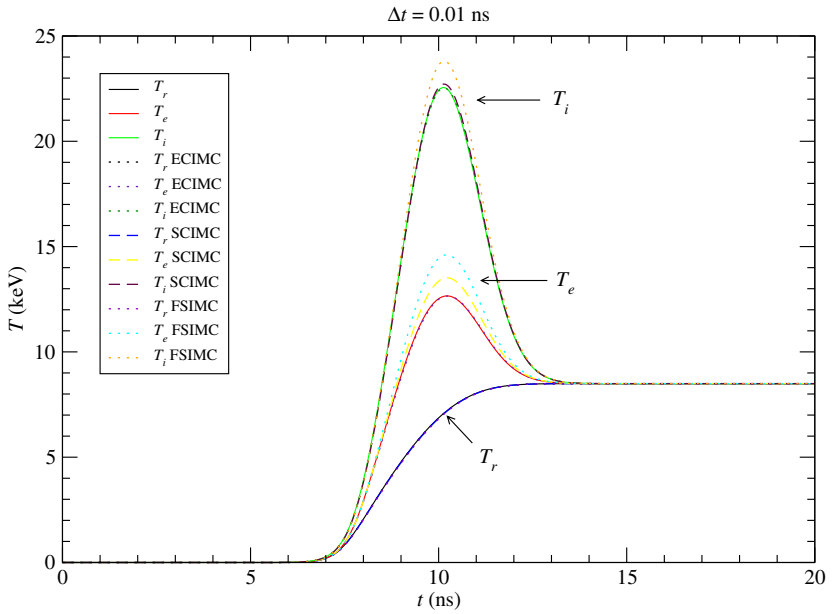

Fig. 1. IMC solutions to the model problem. The timestep is a constant 0.01 ns. The errors in each method as a function of timestep are shown in Fig. 3.

5.2. MEA error calculations

Fig. 2 shows a comparison of the nonlinear, first-order solution of the SCIMC modified equations in (87a)–(87c) and (90a)–(90d) with the SCIMC solution from Eqs. (65a)–(65e) for the model problem. The modified equations reproduce the SCIMC solution. For each IMC method the first-order MEA solution adequately represents the IMC solution. This indicates that we can expect first-order convergence for each method. Plot-

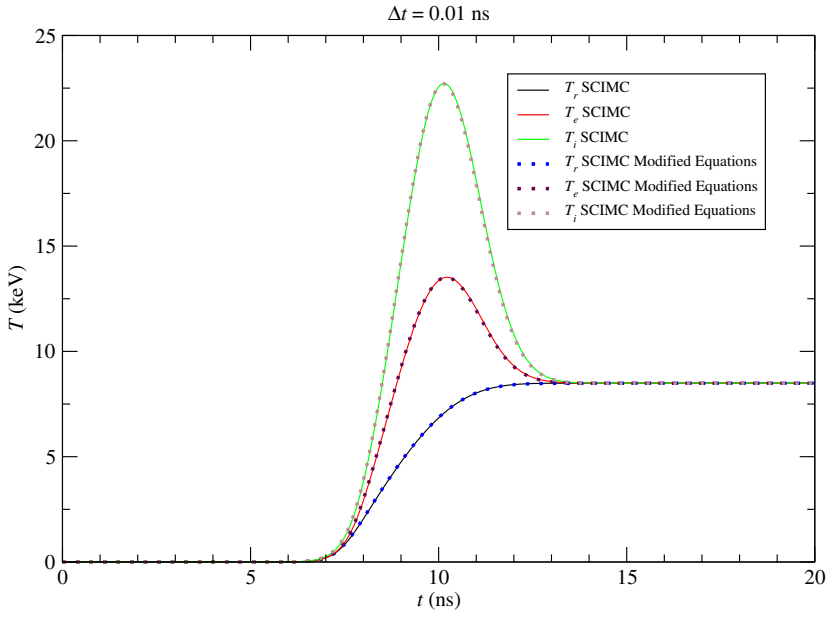

Fig. 2. Comparison of SCIMC solution with corresponding solution to the SCIMC modified equations. The modified equation solution, evaluated non-linearly to first-order, replicates the IMC solution.

ting the L_∞ norms for electron and ion energies for this problem in Fig. 3, we see that the methods do indeed converge to first-order. If the methods did not show first-order convergence, we would have to include higher-order terms in the modified equations to represent the additional errors. Also, the results in Fig. 3 show that the ECIMC method is approximately ten times more accurate than the SCIMC and FSIMC methods for $\Delta t = 0.01$ ns when calculating the electron energy.

We can now use MEA to calculate the errors for each method. Fig. 4 shows the absolute values of the error terms for the model problem (Section 5.1) for each IMC method. Analyzing the error terms in Eqs. (89)–(91) and the results shown in Fig. 4, we see that the SCIMC and FSIMC methods have $\xi_2 \sim \xi_4$. Furthermore, the ECIMC method has very small contributions in the ξ_2 and ξ_4 terms. Labeling the error terms for the SCIMC method as follows

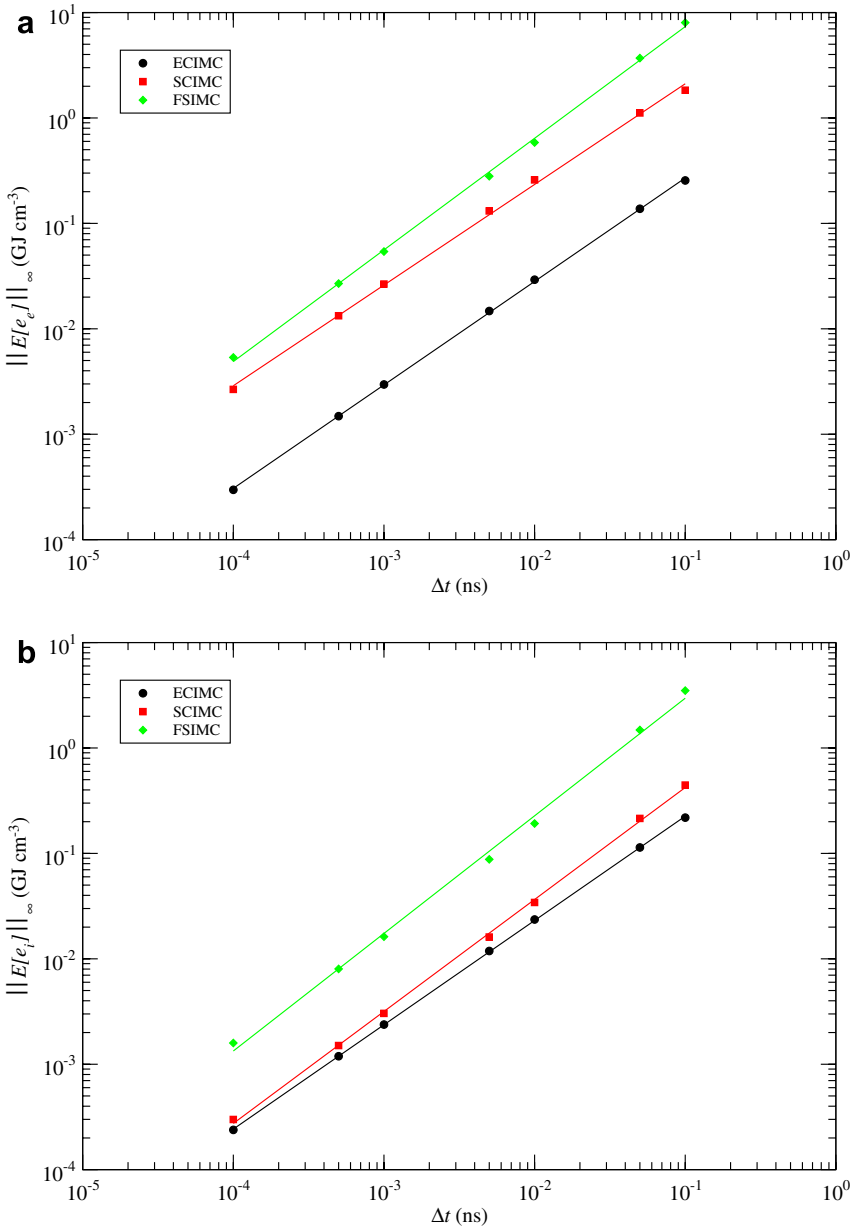

Fig. 3. L_∞ error norms for electron and ion energies. The continuous lines are log-log fits to the data. As indicated by MEA, the methods show first order convergence: (a) electron energy (b) ion energy.

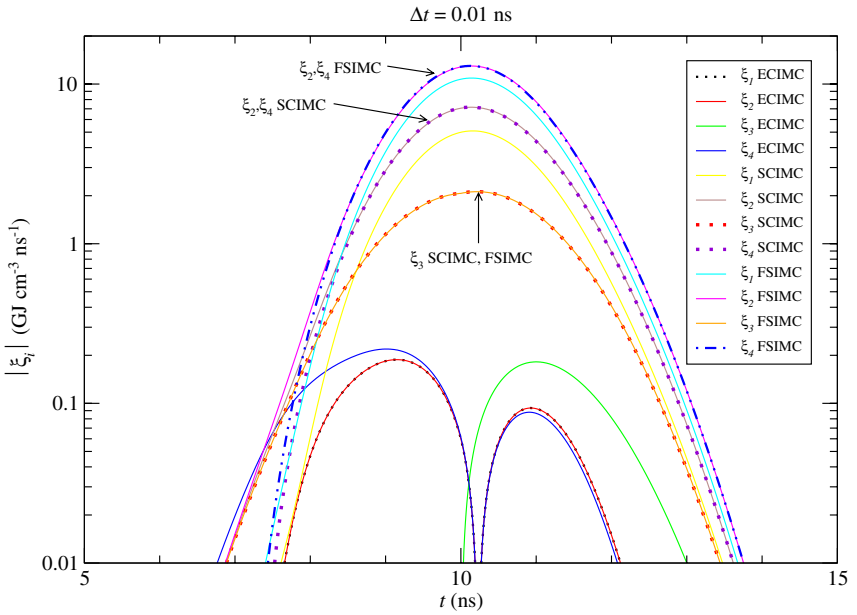

Fig. 4. Error terms generated by MEA for the model problem.

$$\Delta t \frac{C_{ve}}{4\tau^2}\left(\frac{C_{ve}}{C_{vi}}+1\right)(T_i - T_e), \tag{A}$$

$$\Delta t \sigma c \beta \frac{C_{ve}}{2\tau}(T_i - T_e), \tag{B}$$

$$-\frac{1}{\beta}\frac{C_{ve}}{\tau}\frac{\partial \beta}{\partial T_e}(T_e - T_e^n)(T_i - T_e), \tag{C}$$

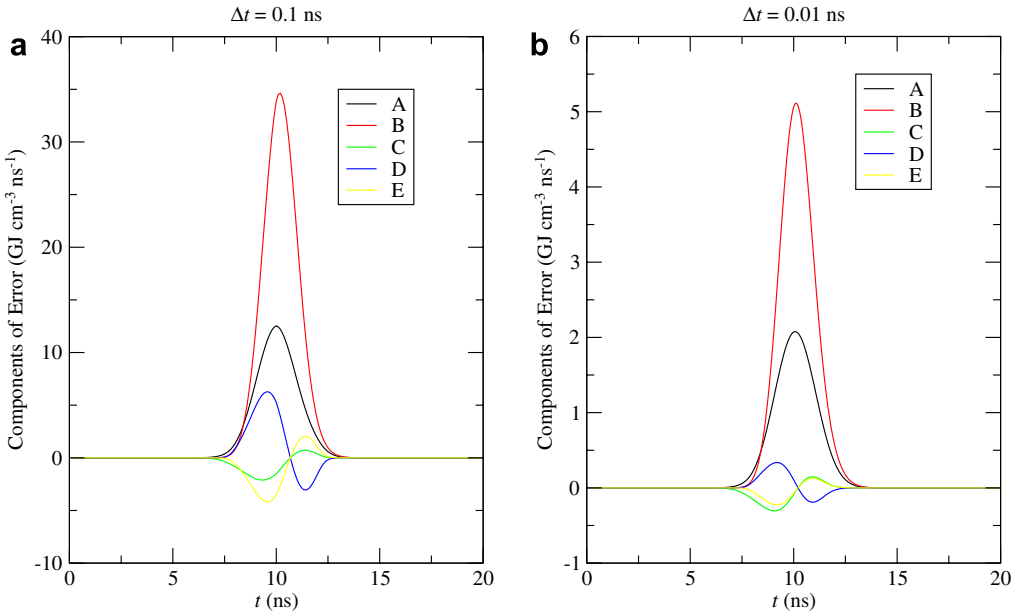

Fig. 5. Components of error for the SCIMC method in the model problem. The A and B components dominate the error; however, as the timestep increases the other terms contribute: (a) $\Delta t = 0.1$ ns; (b) $\Delta t = 0.01$ ns.

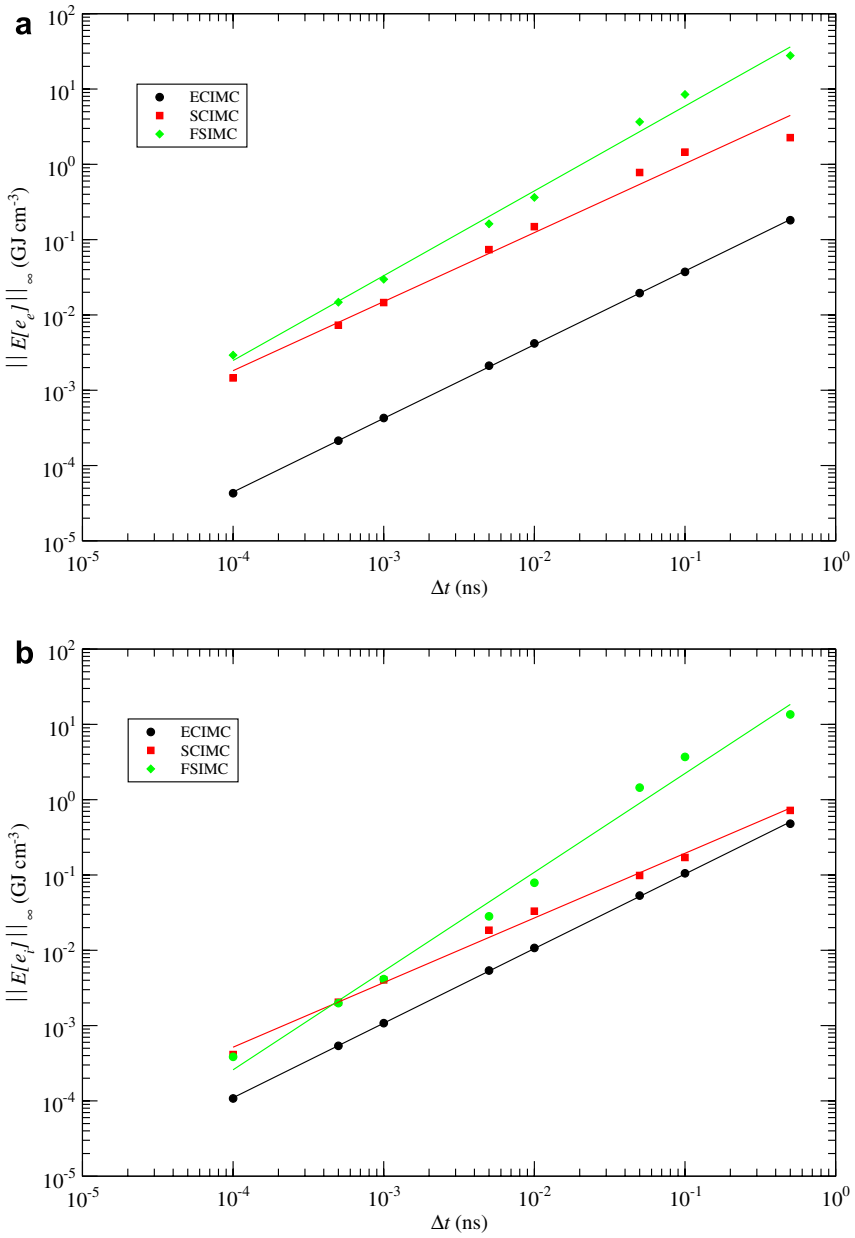

Fig. 6. L_∞ error norms for electron and ion energies with $\sigma_0 = 100$. The continuous lines are log-log fits to the data. Because the B term is unbounded, the SCIMC and FSIMC methods can lose first-order convergence when they do not respect the timescales required by the B error term: (a) electron energy; (b) ion energy.

$$\frac{1}{\beta}\frac{\partial \beta}{\partial T_e}\sigma c(T_e - T_e^n)(\phi - E), \tag{D}$$

$$c\frac{\partial \sigma}{\partial T_e}(T_e - T_e^n)(\phi - E), \tag{E}$$

we conclude that the T_e and ϕ equations are dominated by the A and B error terms. Fig. 5 shows the magnitude of the error terms in Eqs. (90a)–(90d) for $\Delta t = 0.1$ and $\Delta t = 0.01$ ns. Clearly the error is dominated by the A and B terms. These terms do not exist in the ECIMC method, and the B term is twice as large in the FSIMC method. Because the B term is the largest source of error it accounts for the improved accuracy

in the ECIMC and SCIMC methods. Error terms C, D, and E contain time-derivatives of σ and β. These terms become significant when the opacity and temperature are rapidly varying. In the model problem they do not significantly impact the total error.

Error terms C, D, and E will generally be small because of the following limits,

$$\lim_{\sigma\to\infty}(\phi - E) = 0, \tag{93}$$

$$\lim_{\tau\to 0}(T_{\mathrm{i}} - T_{\mathrm{e}}) = 0. \tag{94}$$

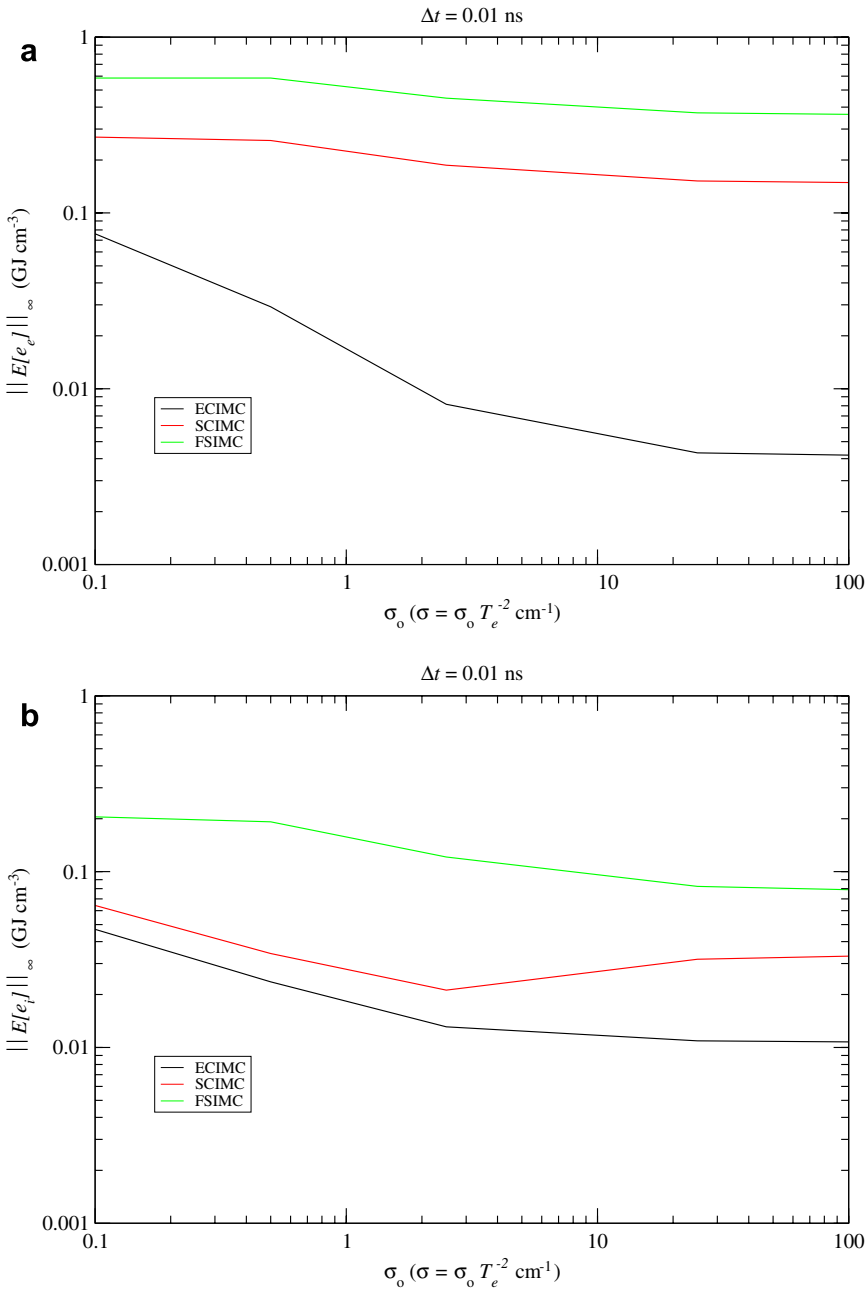

Fig. 7. L_∞ error norms for electron and ion energies as a function of σ_0. Norms are calculated over 0–20 ns problem time: (a) electron energy; (b) ion energy.

When the problem becomes optically thick, error terms D and E vanish. Similarly, when the electrons and ions are tightly coupled C goes to zero. Error term B is not bounded in this manner. This term is proportional to σ, and there is no corresponding radiation–electron coupling term to limit the error when the problem becomes thick. Thus, B represents a source of unbounded error when the electrons and ions are out of equilibrium.

In Fig. 3 we demonstrated that first-order convergence is obtained for all three IMC methods up to time-steps of 0.1 ns. However, the B error term that is present in the SCIMC and FSIMC methods is an unbounded

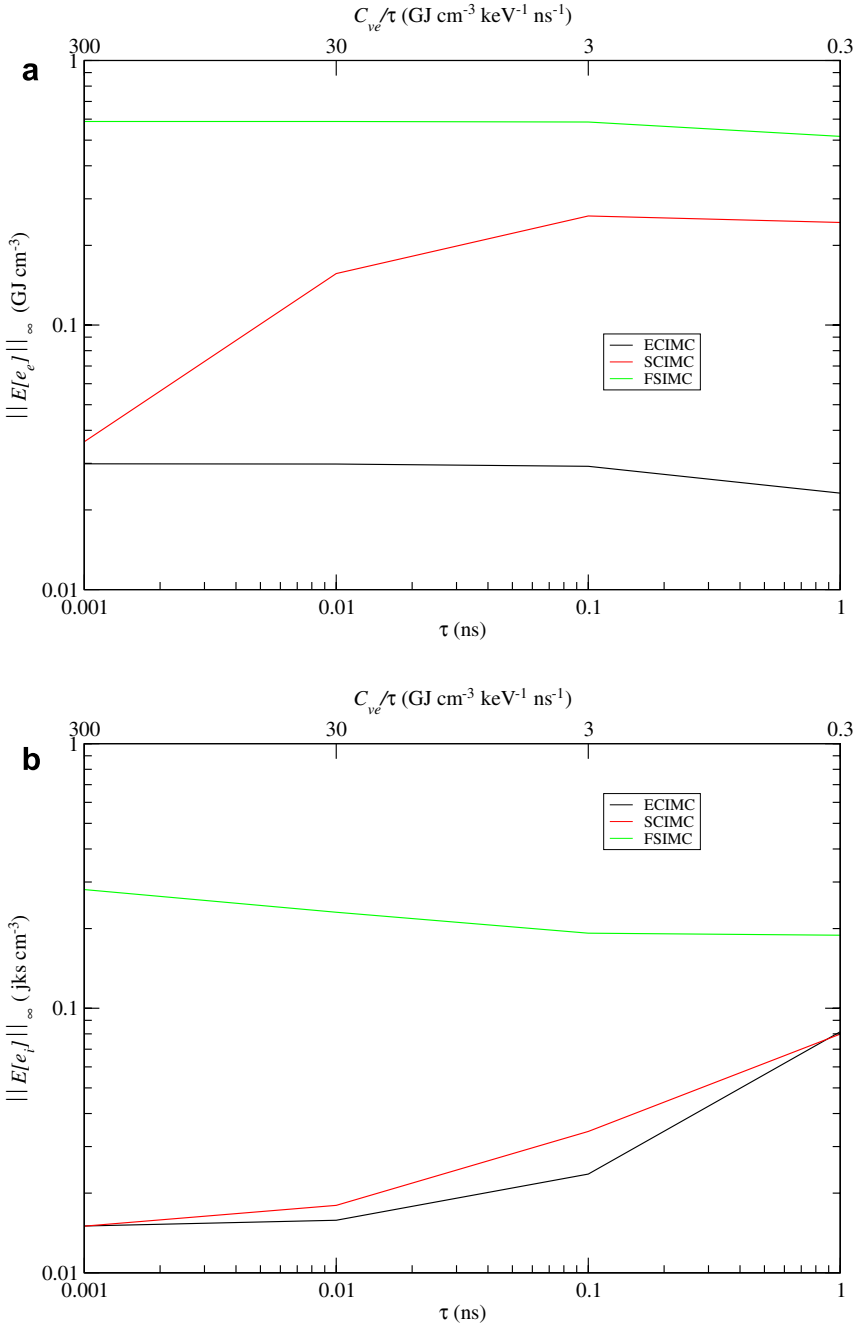

Fig. 8. L_∞ error norms for electron and ion energies as a function of τ and (C_{ve}/τ). Here, $C_{ve} = 0.3$ GJ cm^{-3} keV^{-1}. These parameter studies were run with $\Delta t = 0.01$ ns. Norms are calculated over 0–20 ns problem time: (a) electron energy; (b) ion energy.

function of σ. In Fig. 6 L_∞ error norms are shown for the model problem with $\sigma_0 = 100$. Here we see that the SCIMC and FSIMC methods are no longer first order, and second-order error terms are required in the modified equations in order to match the discrete solutions. When calculating the ion energy, SCIMC begins to lose first-order convergence around $\Delta t = 10^{-2}$ ns, and FSIMC loses first-order convergence around $\Delta t = 5 \times 10^{-3}$ ns. These methods fail first-order convergence because the timescale represented by the coefficient in the B error term is no longer resolved. Since $B \propto \sigma$ the timesteps must be small in thick problems to achieve first-order convergence using the SCIMC and FSIMC methods. Conversely, when the problem is very thick the D and E error terms are zero because $(\phi - E) = 0$. Therefore the ECIMC method maintains first-order convergence independent of σ.

6. Computational parameter studies

Having determined that terms A and B are the principal sources of error that separate the three IMC methods, we can look at the variation of these terms with problem specification. Clearly, as $(A, B) \to 0$ the three methods will yield the same results. Also, all of the error terms (with the exception of the $\dot{Q}_i$ term) are proportional to the separation between electrons and ions, $(T_i - T_e)$, or the separation between electrons and radiation, $(\phi - E)$. We will analyze these effects using the model problem from Section 5.1 as a baseline.

Additionally, our MEA analysis only considered constant τ and C_{ve}. We made this simplification because the analysis becomes hopelessly complex when including nonlinear C_{ve}. Nonetheless, we must consider the effects of nonlinear C_{ve} and τ on each method. These effects are examined in Section 6.4.

6.1. Opacity variation

As discussed in Section 5.2, error term B is proportional to σ; thus, we can expect that ECIMC will perform better than SCIMC and FSIMC as the problem becomes optically thick. Fig. 7 shows L_∞ error norms for each IMC method applied to the model problem with varying σ_0. As expected, ECIMC performs increasingly better than the other methods as the problem gets thicker. For very thick problems, $\sigma_0 \gtrsim 25$, the electron and radiation temperatures do not separate due to the limiting condition in Eq. (93). When this happens the error terms that are proportional to $(\phi - E)$ vanish. The SCIMC and FSIMC errors will be dominated by the A and B terms, where A is roughly constant and B is proportional to σ.

As the problem becomes thin the radiation and electrons can go out of equilibrium because the equilibration time is $(\sigma c)^{-1}$. In these cases, the error terms that are proportional to $(\phi - E)$ will dominate. These terms are present in all three IMC methods.

6.2. Electron–ion coupling variation

Error terms A, B, and C are proportional to (C_{ve}/τ), so we need to analyze the effect of this parameter on the accuracy of the methods. Interpretation of the results is difficult because error terms that are proportional to $(T_i - T_e)$ are inversely proportional to τ. Thus, the effect of τ is related to the rate at which $(T_i - T_e) \to 0$ versus the magnitude of (C_{ve}/τ).

Fig. 8 shows the L_∞ norms for electron and ion energies as a function of τ and (C_{ve}/τ) for all three IMC methods. As indicated in the figure, the ECIMC method performs better than the other methods; however, we cannot make easy characterizations about the affect of this parameter because of the conflict between the ion–electron separation and the magnitude of τ. One observation is that the electron energy errors are significantly greater for the SCIMC and FSIMC methods at large τ, whereas the ion energy errors are nearly the same for the ECIMC and SCIMC methods at large τ.

6.3. Ion source variation

The model problem uses a fitted Gaussian with a peak of 30.0 GJ cm^{-3} ns^{-1}. The magnitude of the ion source (Q_i) will strongly affect the ion–electron separation as shown in Table 1. Fig. 9 shows the L_∞ norms for electron and ion energies as a function of the peak ion source strength. When the source is small there

Table 1
Maximum ion–electron temperature difference for varying peak source strengths

Q_{peak} (GJ cm^{-3} ns^{-1})	max $\lvert T_i - T_e \rvert$ (keV)
0.3	0.068
3.0	0.941
15.0	4.938
30.0	9.931

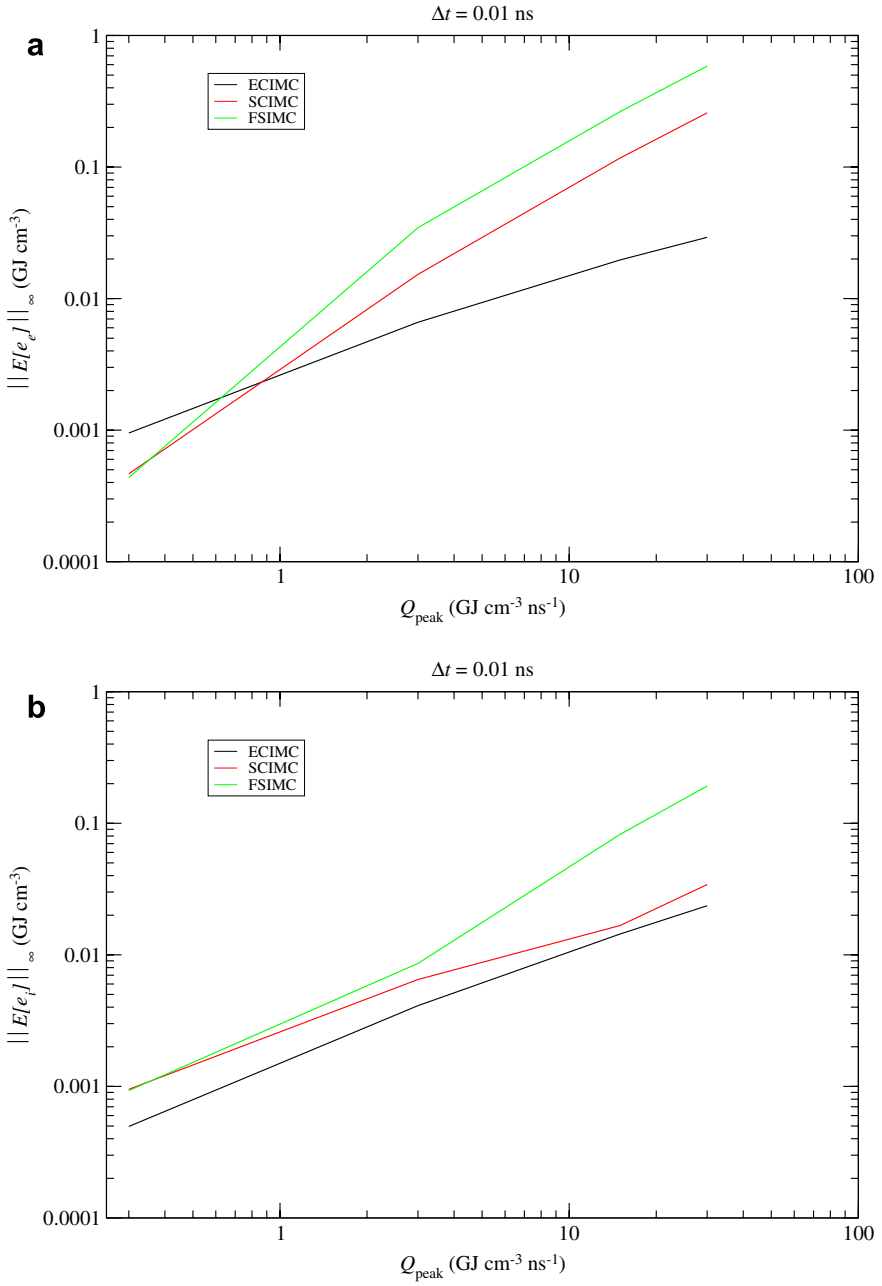

Fig. 9. L_∞ error norms for electron and ion energies as a function of the peak Gaussian ion source strength. Norms are calculated over 0–20 ns problem time: (a) electron energy; (b) ion energy.

is very little separation in the ion and electron temperatures, and all of the methods will be accurate. As the source strength increases the ions and electrons will go out of equilibrium causing the A and B error components in the SCIMC and FSIMC methods to grow. Thus, the ECIMC method performs better in problems with sources that cause the electrons and ions to separate.

6.4. Nonlinear EOS

Thus far we have only considered linear variations in EOS and material data, namely C_{ve}, C_{vi}, and τ. We must consider the effect of nonlinear C_{ve} on the performance of each method. Because the MEA only considered constant EOS we will perform this analysis heuristically with a variation of the model problem that admits $C_{ve} \propto T_e$ [10]. The problem we shall consider has the following specification:

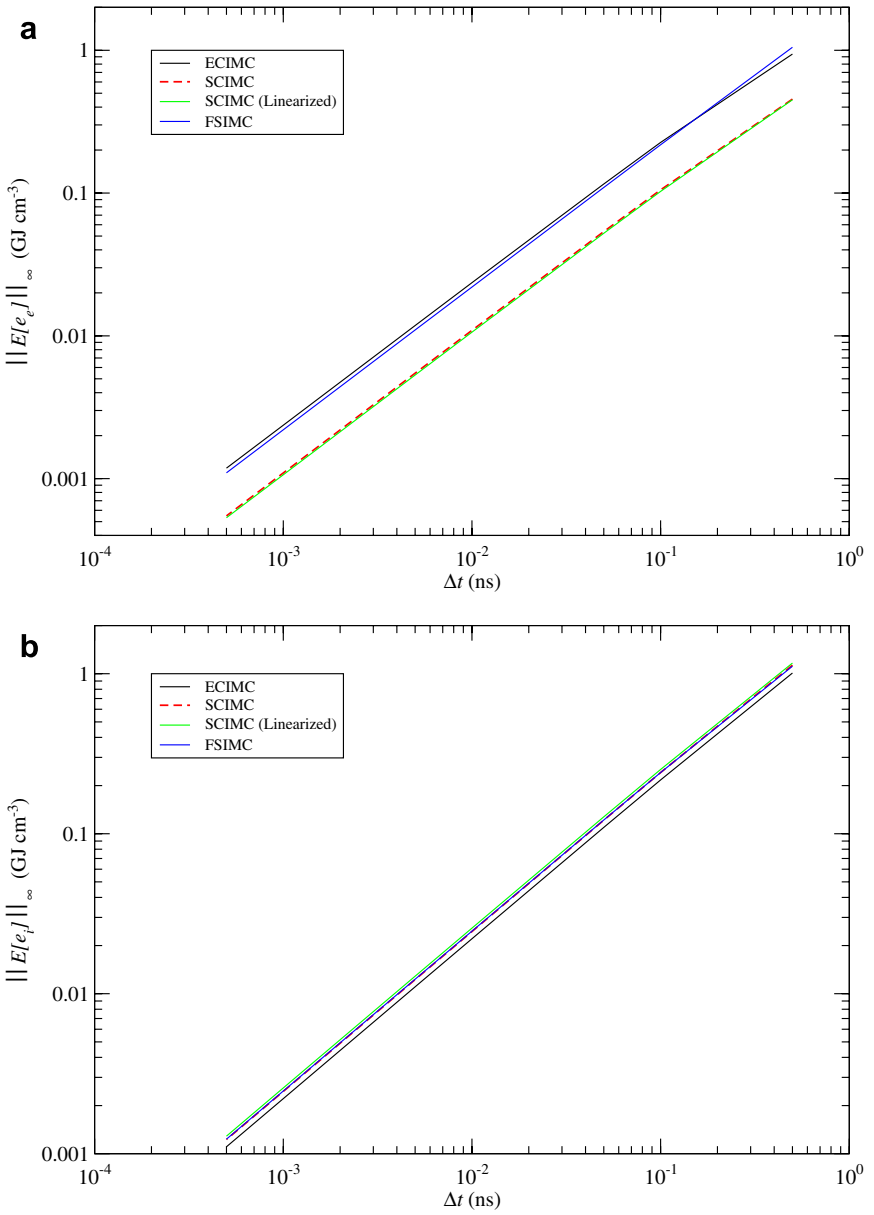

Fig. 10. L_∞ error norms for electron and ion energies. Results are shown for solving split **III** of the SCIMC method using nonlinear Newton iteration and linearization as shown in Eqs. (65d) and (65e): (a) electron energy; (b) ion energy.

$\mathfrak{C} = 5.01326$

$\sigma_0 = 0.1$

$C_{ve} = 0.1\rho T_e$ [GJ cm^{-3} keV^{-1}]

$\tau = 0.72521 T_e^{3/2}$ ns

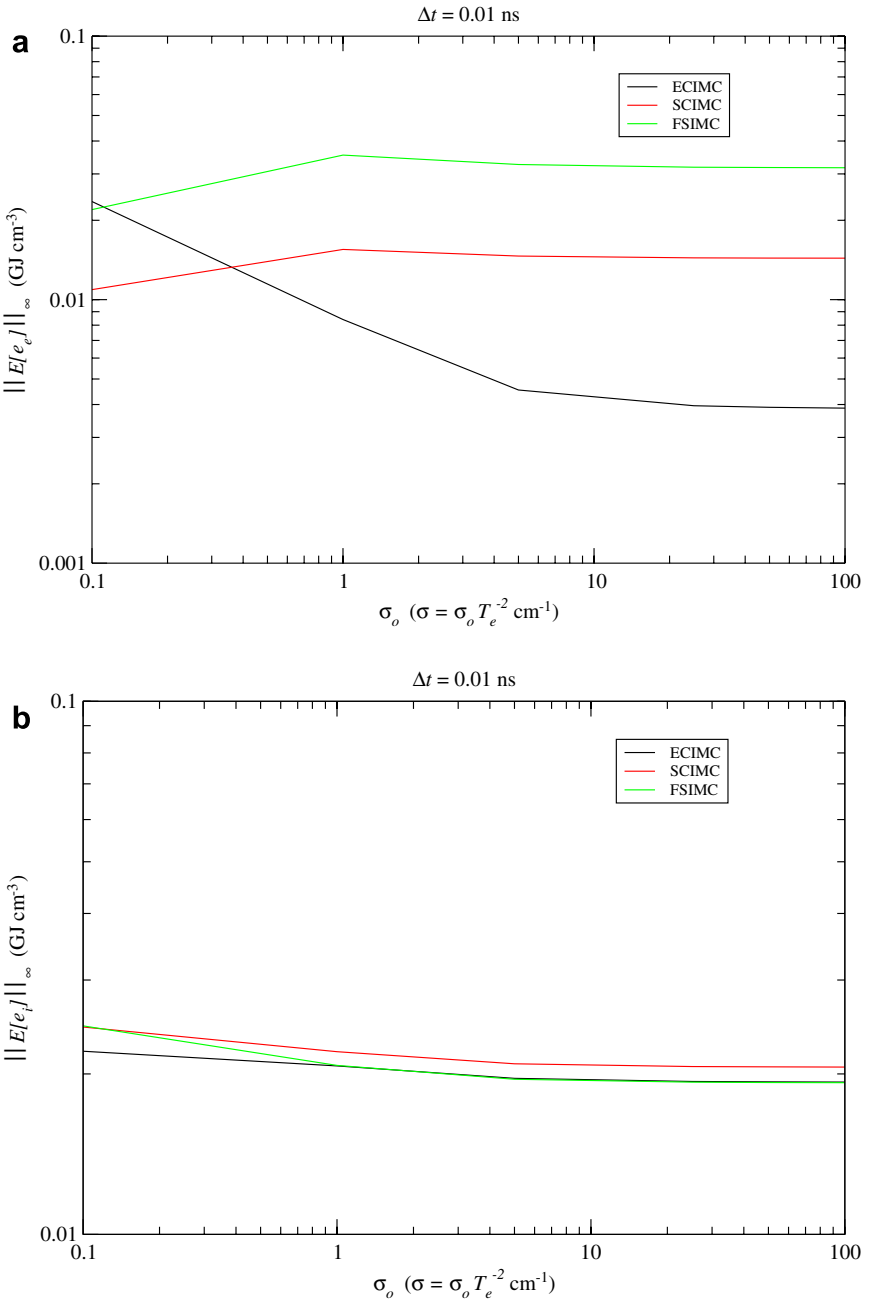

Fig. 11. L_∞ error norms for electron and ion energies as a function of σ with nonlinear C_{ve}. SCIMC solutions are generated with nonlinear Newton iteration for split **III**: (a) electron energy; (b) ion energy.

All other initial conditions are identical to the model problem. The model for τ is given in Eq. (5). For this problem we set $\lambda = 15$. The number density of electrons and ions are equivalent, $n_e = n_i = n$, and $n \approx 10^{18}$ cm^{-3} for dense, hot plasmas.

Fig. 10 shows L_∞ error norms for electron and ion energy versus timestep for each IMC method. Here, we see that the SCIMC method performs best followed by the FSIMC method for calculating the electron energy. All of the methods are equally accurate when calculating the ion energy. There is a straightforward reason for this result. Because the SCIMC and FSIMC methods have more electron-energy splits than the ECIMC method, the temperature variation on internal energy will be more accurately represented over the timestep. For example, in ECIMC the coupling effect on internal energy is done with the beginning timestep temperature. In SCIMC and FSIMC the temperature-variation in the EOS is applied multiple times during the solve. The ECIMC scheme only integrates C_{ve} once per timestep, and therefore, the integration error will be greater for this method when C_{ve} has strong dependence on T_e. We also note that solving split **III** in the SCIMC method with a fully nonlinear method (Newton iteration) yields nearly identical results to the linearized solve.

The EOS integration error is small compared to the error terms resulting from the splits in the SCIMC and FSIMC methods. The problem we just considered is very thin, $\sigma = 0.1T_e^{-2}$. If this same problem is run with varying σ the errors resulting from the additional splits in the SCIMC and FSIMC methods quickly overwhelm the EOS integration error as $\sigma \to \infty$. The results for this problem are illustrated in Fig. 11. As the problem becomes thick the ECIMC scheme gives the most accurate results.

7. Conclusions

We have analyzed three IMC methods for performing 3T transport calculations. Using MEA we have shown that, for the simplified system in Eqs. (58a)–(58c), the ECIMC method has the smallest number of error terms. Also, in Section 6 we have demonstrated that ECIMC is consistently the most accurate of the three methods. However, in thin problems with small ion–electron temperature separation, the SCIMC method is competitive. We will continue to investigate these problems in a future paper. We may find that the SCIMC method has advantages in thin problems that has large contributions from electron or ion conduction, which we have not yet analyzed.

In problems where the effects of conduction can be ignored, the ECIMC method is the obvious choice. The only other realistic competitor would be a variant of the FSIMC method in which the electron–ion coupling was calculated in a single solve. However, MEA shows that the unbounded error term B is still present in this scheme. When conduction can be neglected, ECIMC is the most accurate method.

All of the IMC methods presented in this work are first-order accurate in time. However, the SCIMC and FSIMC methods have more significant timestep constraints due to the presence of unbounded error terms that result from the splitting. These terms are proportional to σ; thus, we can expect that the timestep constraints will be more severe in the SCIMC and FSIMC methods in thick problems. The ECIMC error terms are bounded so it maintains first-order convergence as long as the dynamic timescale of the problem is respected.

The first-order results obtained in this work resulted from deterministic solutions of the Monte Carlo solutions. In practical Monte Carlo simulations statistical errors often overwhelm discretization errors. This fact has strong implications for the possibility of developing second-order Monte Carlo methods. We expect that the statistical variance in the solution will prevent second-order convergence. In addition, second-order methods that preserve positive unknowns require iteration. Because of efficiency constraints and statistical noise, iterative methods are not feasible in real Monte Carlo calculations. Second-order methods that do not require iteration exist; for example, Rosenbrock schemes give second-order convergence without iteration [11]. However, these methods are based on an estimate of the residual that can be negative. Negative weights are best avoided in Monte Carlo simulations because they increase the variance of the solution. Second-order Monte Carlo methods are an area of future research, but the state-of-the-art is still first order.

While we have not performed detailed performance analysis, we can state that the ECIMC method is the least expensive scheme from the standpoint of number-of-operations. Both the SCIMC and FSIMC methods require two inversions of the parabolic conduction operator. SCIMC requires one sweep of the mesh to solve split **III**. FSIMC requires this sweep plus an additional sweep to solve split **Ib**. When Newton's method, or another nonlinear iteration scheme, is used to solve these splits, multiple iterations per cell will be required

on the block-diagonal matrix that constitutes split **III**. Monte Carlo performance analysis on these methods will be the topic of a future paper.

Finally, we have not analyzed the effects that conduction has on the proposed IMC methods. The splittings proposed in this paper impose error from the treatment of conduction. Nonetheless, these additional errors do not invalidate the analysis of errors resulting from the electron–ion coupling splits and linearization of the radiation equation. Therefore, we feel justified in analyzing the errors in the linearization and splitting schemes that we have proposed in this paper while neglecting conduction. We will investigate problems with conduction using fully implemented Monte Carlo solvers in a future study.

The next stage of this work will integrate the methods presented here in a Monte Carlo code. We will investigate the effect that the conduction treatment imposes on each method. We will also analyze frequency-dependence, which has been neglected in this analysis.

Acknowledgments

We thank Drs. Dana Knoll and Rob Lowrie for useful discussions during this study. We also thank Dr. Ed Larsen for proofreading the manuscript and providing useful comments. This work was performed under US government contract DE-AC52-06NA25396 for Los Alamos National Laboratory, which is operated by Los Alamos National Security, LLC. (LANS) for the US Department of Energy.

References

[1] J.A. Fleck, J.D. Cummings, An implicit Monte Carlo scheme for calculating time and frequency dependent nonlinear radiation transport, Journal of Computational Physics 8 (3) (1971) 313–342.
[2] M. Sincell, M. Gehmeyr, D. Mihalas, The quasi-stationary structure of radiating shock waves. II. The two-temperature fluid, Shock Waves 9 (1999) 403–411.
[3] J. Huba, NRL Plasma Formulary, Naval Research Laboratory, Washington, DC, 2004.
[4] G. Olson, J.E. Morel, Solution of the radiation diffusion equation on an AMR Eulerian mesh with material interfaces, Internal Report LA-UR-99-2949, June 1999.
[5] T.D. Matteo, E. Blackman, A. Fabian, Two-temperature coronae in active galactic nuclei, Monthly Notices of the Royal Astronomical Society 291 (1997) L23–L27.
[6] D. Griffiths, M. Sanz-Serna, On the scope of the method of modified equations, SIAM Journal of Scientific and Statistical Computing 7 (3) (1986) 994–1008.
[7] D. Knoll, L. Chacon, L. Margolin, V. Mousseau, On balanced approximations for time integration of multiple time scale systems, Journal of Computational Physics 185 (2003) 583–611.
[8] J.A. Fleck Jr., E.H. Canfield, A random walk procedure for improving the computational efficiency of the Implicit Monte Carlo method for nonlinear radiation transport, Journal of Computational Physics 54 (1984) 508–523.
[9] M. Gehmeyr, D. Mihalas, Adaptive grid radiation hydrodynamics with TITAN, Physica D 77 (1994) 320–341.
[10] Y.B. Zel'dovich, Y.P. Raizer, Physics of Shock Waves and High-Temperature Hydrodynamic Phenomena, Academic Press, New York, 1966.
[11] R. Lowrie, A comparison of implicit time integration methods for nonlinear relaxation and diffusion, Journal of Computational Physics 196 (2004) 566–590.